

Dear Editor,

On behalf of my co-authors, I'm submitting our revised manuscript for possible publication in "Atmospheric Chemistry and Physics".

Thank you very much for your great efforts and high efficiency on evaluating our submission. We would also like to sincerely thank three anonymous reviewers for their constructive comments which are very helpful for us to improve our manuscript. We have carefully considered and fully addressed all comments. Below are the detailed point-by-point responses to the review comments. For clarity, the referees' comments are listed in black italics, while our responses and changes in the manuscript are shown in blue. We also mention where we make necessary changes in the revised manuscript by indicating page and line numbers in our responses. The marked manuscript was also uploaded to be easily reviewed.

We look forward to hearing from you soon.

Yours truly,

Lei Zhong et al.

## **Response to Reviewer #1**

*Observations of land surface heat fluxes over the QTP are essential for understanding the land-atmosphere interactions. However, limited by the small amount of land-atmosphere monitoring stations and sparse spatial coverage, it is difficult to quantify the responses of the land-atmosphere interactions under the condition of climate warming on the QTP. This study aims to provide a plateau-scale product with a notable advantage of hourly-resolution using the SEB model in conjunction with the observations from polar and geostationary satellites. As we know that the temporal resolution of land surface heat fluxes is highly dependent on the forcing in various modelling approaches. In general, temperature and wind speed are two key input variables for the latent heat flux and the turbulent flux, respectively. The input variables in this study use the hourly temperature observations and other observations with a three-hour resolution. As a result, the reliability of the turbulent flux might be problematic when using the energy balance equation for calculation, and its accuracy is even worse than the 3-hourly product using data assimilation approach (e.g., GLDAS). A rigorous analysis of the accuracy is required to consolidate the proposed method. Given the present analysis, the current conclusion of hourly-resolution is not convincing for me. Considering other issues, a substantial revision is needed for this manuscript.*

**Author Response:** We would like to thank Reviewer #1 for the insightful and constructive comments. All your comments and suggestions are very helpful for improving our manuscript. We have carefully considered and addressed all of these comments, and significantly revised our manuscript. Please find our point-by-point response below.

### **Major issues:**

- (1) *Since forcing data is lack of homogeneity in temporal and spatial resolution, the authors should discuss their impacts on the accuracy of the product. The authors claimed a spatial resolution of 5 km, but it has been changed to 10 km in the new version (no rational explanation in the text). I think the authors should cope with the similar problem for the temporal resolution. As mentioned above, the methodology needs a rigorous analysis of the accuracy of the estimated land surface fluxes. Besides, I did not find the description of how to use the 3 hour-forcing in the SEBS model to produce the hourly product.*

**Author Response:** Thank you for the above comments. The lack of homogeneity in the temporal and spatial resolution, mainly exists in the meteorological forcing data because its spatial and temporal resolution are lower than those of other satellite derived inputs. In addition to some remarks about this issue in Section 5 (P11, L27-30; P12, L1-4), we also performed some sensitivity tests to verify how the RMSEs of forcing data can affect the sensible heat flux and latent heat flux. As shown in Figure 4, three sites located in the northern, western and southeastern part of the TP were randomly selected to perform the sensitivity analysis. All input meteorological forcing parameters in Table 3 ( $R_{swd}$ ,  $R_{lwd}$ ,  $u$ ,  $T_a$ , SH,  $P_s$ ) are selected. The original sensible heat flux and latent heat flux from the SEBS model are used as reference values. The RMSEs of different forcing data were used as perturbations. As shown in Table 5, the sensible heat flux is highly sensitive to  $R_{swd}$ ,  $u$  and  $T_a$ , while the latent heat flux is very sensitive to  $R_{swd}$ ,  $R_{lwd}$  and  $T_a$ . Both sensible heat flux and latent heat flux are not sensitive to errors of SH and  $P_s$ . As the  $R_{swd}$  has a variation from  $-68.5 \text{ Wm}^{-2}$  to  $68.5 \text{ Wm}^{-2}$ , the induced latent heat flux uncertainty ranges from  $-29.75 \text{ Wm}^{-2}$  to  $35.86 \text{ Wm}^{-2}$ . Similarly, the sensible heat flux is very sensitive to  $T_a$ . When  $T_a$  has an uncertainty from  $-2.08 \text{ K}$  to  $2.08 \text{ K}$ , the induced sensible heat flux uncertainty ranges from  $14.64 \text{ Wm}^{-2}$  to  $-16.94 \text{ Wm}^{-2}$ . All the above works has been added to the revised manuscript. (P9, L6-16)

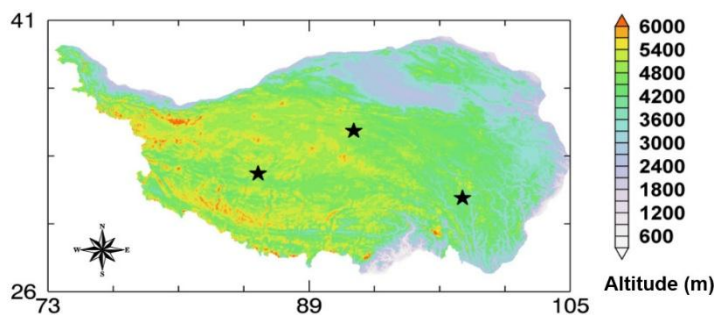


**Figure 4: Locations of the three sites (marked by pentagrams) used to carry out sensitivity tests of the meteorological forcing input data. The legend of the color map indicates the elevation above mean sea level in meters.**

**Table 5: Uncertainties for each meteorological forcing variable and the induced changes for  $H_s$  and LE.**

Variables	Assumed Uncertainty	Induced Uncertainty of $H_s$	Induced Uncertainty of LE
$R_{swd} (\text{W}\cdot\text{m}^{-2})$	$-68.50\sim68.5$	$-12.34\sim6.22$ ( $-8.05\%\sim4.06\%$ )	$-29.75\sim35.86$ ( $-17.92\%\sim21.60\%$ )
$R_{lwd} (\text{W}\cdot\text{m}^{-2})$	$-20.98\sim20.98$	$-2.50\sim2.50$ ( $-1.63\%\sim1.63\%$ )	$-15.54\sim15.54$ ( $-9.36\%\sim9.36\%$ )

$u$ ( $\text{m} \cdot \text{s}^{-1}$ )	-1.71~1.71	-9.47~7.31 (-6.18%~4.77%)	9.47~7.31 (5.71%~4.41%)
$T_a$ (K)	-2.08~2.08	14.64~16.94 (9.55%~11.05%)	-14.64~16.94 (-8.82%~10.20%)
SH ( $\text{kg} \cdot \text{kg}^{-1}$ )	$-0.56 \times 10^{-3}$ ~ $0.56 \times 10^{-3}$	-0.01~0.01 (-0.01%~0.01%)	0.01~0.01 (0.01%~0.01%)
$P_s$ (hPa)	-8.51~8.51	-0.01~0.01 (-0.01%~0.01%)	0.01~0.01 (0.01%~0.01%)

The spatial resolution of the final flux products should be determined by the lowest input of the source data, which was mentioned in the revised manuscript (P5, L8-9). Thus, the final surface heat flux product should be 10 km. We have corrected this mistake in the manuscript after the quick review and mentioned this issue in the response letter to the quick reviewer comments.

For the temporal resolution, a linear statistical downscaling method was used to derive the hourly meteorological forcing data based on the original 3-hour forcing data and in situ measurements in this study. The general idea is to establish an empirical relationship between each 3-hour in situ measurement. Then, this relationship is applied to meteorological forcing data (P5, L17-21). For example,  $T_{a00}$ ,  $T_{a01}$  and  $T_{a03}$  represent the in situ air temperature measurements from six stations at 00h, 01h and 03h, respectively. Thus  $T_{a00} = [a_1, a_2, a_3, a_4, a_5, a_6]$ ,  $T_{a01} = [b_1, b_2, b_3, b_4, b_5, b_6]$ , and  $T_{a03} = [c_1, c_2, c_3, c_4, c_5, c_6]$ . Then, the linear equation  $T_{a01} = k_1 T_{a00} + k_2 T_{a03}$  can be solved. According to the meteorological forcing data at 00h and 03h, the plateau scale  $T_a$  at 01h can be achieved by the following formula.

$$\begin{pmatrix} b_{11} & \cdots & b_{1n} \\ \vdots & \ddots & \vdots \\ b_{m1} & \cdots & b_{mn} \end{pmatrix} = k_1 \begin{pmatrix} a_{11} & \cdots & a_{1n} \\ \vdots & \ddots & \vdots \\ a_{m1} & \cdots & a_{mn} \end{pmatrix} + k_2 \begin{pmatrix} c_{11} & \cdots & c_{1n} \\ \vdots & \ddots & \vdots \\ c_{m1} & \cdots & c_{mn} \end{pmatrix}$$

where  $a$ ,  $b$  and  $c$  represent meteorological forcing data at 00h, 01h and 03h respectively; and  $m$  and  $n$  represent total rows and columns, respectively, of the grid data. The meteorological forcing data at other times can be achieved similarly determined.

(2) *The major supporting for the conclusion of a better performance of the proposed product than the GLDAS produce is based on the comparison with the observational data. The authors use the Bowen ratio calibration method to improve the observed data. We know the validity of the Bowen ratio method varies distinctly in different environments due to the different fulfillment of assumptions. As a result, certain biases will be brought into the*

*observational data, and this can mislead the comparison. First, it is not clear in the text that if the comparison is under the same condition that the observational data are all corrected with the Bowen ratio method. Second, even if using the similar observational data for the comparison, the biases from the correction can still distort the RMSE. Hence, I would suggest directly using the observed data for comparison. Besides, since the data quality of eddy covariance measurements may vary at the 6 stations, comparison on the indicators like RMSE at each station separately may provide more information.*

**Author Response:** It should be noted that the in situ flux data have been flagged by steady state tests and developed conditions tests according to Foken and Wichura (1996) and Foken et al. (2004). Steady conditions mean that all statistical parameters do not vary with time. The flux-variance similarity was used to test the development of turbulent conditions. A data quality of only QA<5 was chosen to make the comparison. Therefore, the comparison is under similar conditions. The above information has been included in the text (P7, L27-28; P8, L1-2).

The Bowen ratio correction method was only used to correct the in situ latent heat flux measurements and was not used for the other three energy balance components (radiation heat flux, sensible heat flux and soil heat flux). The following equation was used to perform the Bowen ratio correction.

$$BRLE = \frac{1}{1 + \beta} (R_n - G_0)$$

where  $BRLE$  is the latent heat flux after correction and Bowen ratio  $\beta = \frac{H}{LE}$ .  $R_n$  and  $G_0$  are net radiation flux and soil heat flux, respectively.

As you mentioned, the validity of the Bowen ratio method varies distinctly in different environments due to the different assumptions. We try to use the original latent heat flux measurements to perform the validation. The following figure shows the comparison between surface latent heat fluxes estimated by the SEBS model with in situ measurements. All corresponding values for the latent heat flux comparison have been replaced in Table 4 (P18). It can be seen that that indicators for latent heat flux have been changed but the they will not influence the general results of this paper. All information on the Bowen ratio correction has been deleted from the original manuscript.

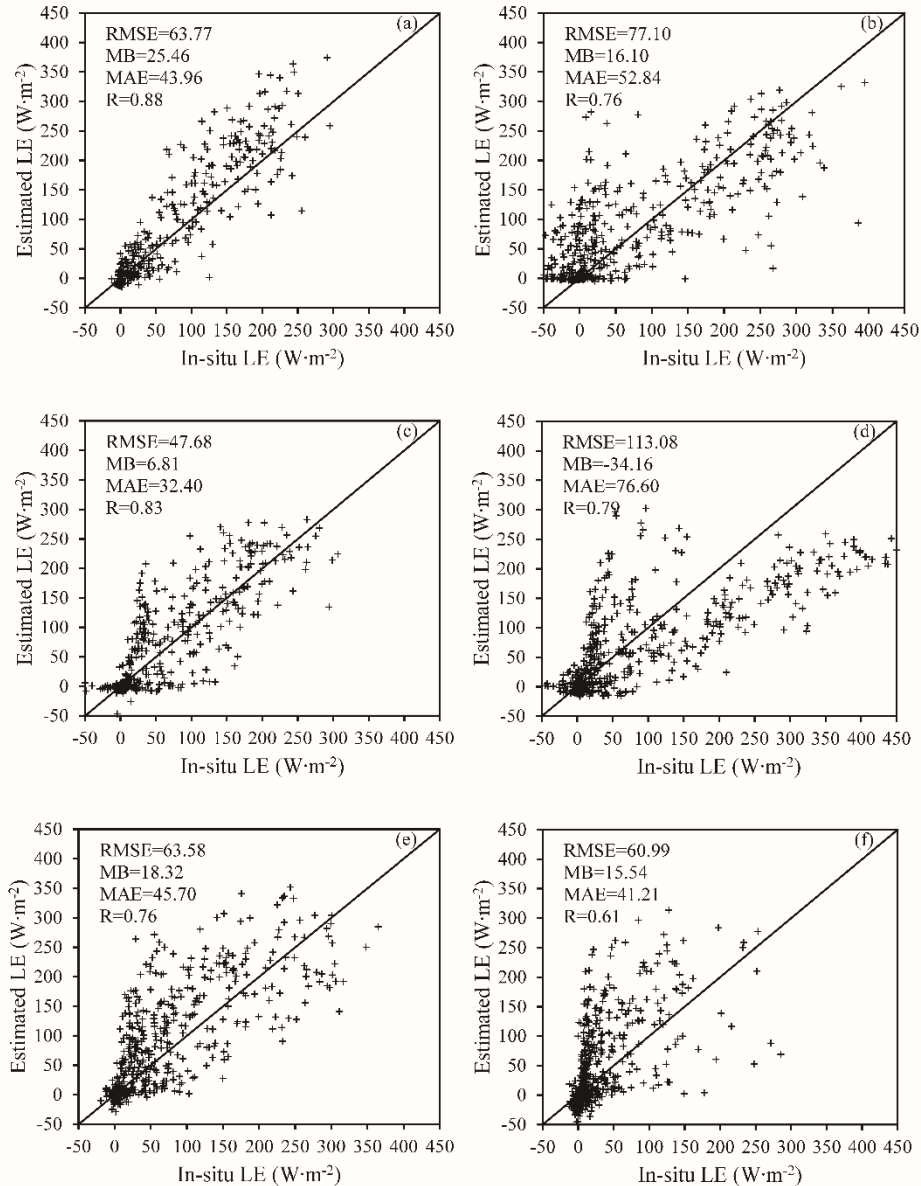


**Figure: Validation of surface latent heat fluxes estimated by the SEBS model with in situ measurements (a. BJ station; b. D105 station; c. Linzhi station; d. MS3478 station; e. Nam Co station; f. QOMS station).**

For your last question, since the data quality of eddy covariance measurements may vary at the 6 stations, a separate comparison of the indicators, such as RMSE, at each station may provide more information. For the data quality, QA<5 was chosen to ensure the flux measurements are under similar steady state and developed conditions; thus, it is not necessary to make a comparison at each station separately. There will be some differences among those stations, but most of these differences can be explained by the quality of the input forcing data, as shown in the sensitivity test.

(3) *The product provided by the authors is produced based on the input data with a spatial resolution no less than 10 km. The authors compare it with a product with a spatial resolution of 25 km. While the scale of the stations normally represents a scale of about less than 1 km. The authors should give some explanation about their comparability.*

**Author Response:** The scale problem you mentioned is an important and difficult problem to be solved in the quantitative remote sensing and atmospheric research field. First, the datasets generated by our methods need to be validated by comparison with the observation dataset. The eddy covariance system is widely accepted as a direct measurement of energy heat fluxes and has been used to validate satellite estimations (Fisher et al, 2008, Ma et al, 2006, Su 2002). Some errors can be caused due to scale mismatch among the stations between the SEBS product and GLDAS product. This issue has been discussed in Section 4.1 (P9, L16-19) and Section 5. Because of the relatively homogeneous land surface conditions of the field stations, this effect should have been minimized in our study. Scintillometry is possibly the most convenient method to measure fluxes at a 1-10 km scale. Unfortunately, this device is lacking over the TP. If we have enough in situ measurements within a grid scale of 10 km or 25 km, an average or weighted average of the measurements can be directly used to reduce some uncertainties caused by scale mismatch. However, for well-known reasons, it is very difficult to carry out such measurements in the TP with the harsh environment and climate conditions. The above discussions have been added to the revised manuscript. (P11, L27-30; P12, L1-4)

### **Minor issues:**

(1) *P5-line 13-25: the authors validate the forcing data and find the notable variance. These differences can further propagate to the product. Please discuss its relation to the final product.*

**Author Response:** Yes, we totally agree with you. According to your suggestion, a sensitivity test was carried out to test how the RMSE of forcing data can affect the sensible heat flux and latent heat flux. As shown in Figure 4, three sites located in the northern, western and southeastern part of the TP were randomly selected to perform the sensitivity analysis. All input meteorological forcing parameters in Table 3 ( $R_{swd}$ ,  $R_{lwd}$ ,  $u$ ,  $T_a$ , SH,  $P_s$ ) are selected. The original sensible heat flux and latent heat flux from the SEBS model are used as reference values. The RMSEs of different

forcing data were used as perturbations. As shown in Table 5, the sensible heat flux is highly sensitive to  $R_{swd}$ ,  $u$  and  $T_a$ , while the latent heat flux is very sensitive to  $R_{swd}$ ,  $R_{lwd}$  and  $T_a$ . Both sensible heat flux and latent heat flux are not sensitive to errors of SH and  $P_s$ . As  $R_{swd}$  varies from  $-68.5 \text{ Wm}^{-2}$  to  $68.5 \text{ Wm}^{-2}$ , the induced latent heat flux uncertainty ranges from  $-29.75 \text{ Wm}^{-2}$  to  $35.86 \text{ Wm}^{-2}$ . Similarly, the sensible heat flux is very sensitive to  $T_a$ . When  $T_a$  has an uncertainty from  $-2.08 \text{ K}$  to  $2.08 \text{ K}$ , the induced sensible heat flux uncertainty ranges from  $14.64 \text{ Wm}^{-2}$  to  $-16.94 \text{ Wm}^{-2}$ . All the above information has been added to the revised manuscript. (P9, L6-16)

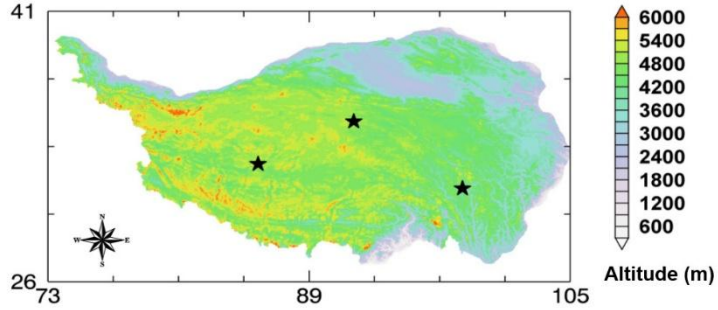


**Figure 4:** Locations of the three sites (marked by pentagrams) used to carry out sensitivity tests of the meteorological forcing input data. The legend of the color map indicates the elevation above mean sea level in meters.

**Table 5: Uncertainties for each meteorological forcing variable and the induced changes in  $H_s$  and LE.**

Variables	Assumed Uncertainty	Induced Uncertainty of $H_s$	Induced Uncertainty of LE
$R_{swd} (\text{W}\cdot\text{m}^{-2})$	$-68.50\text{--}68.5$	$-12.34\text{--}6.22$ ( $-8.05\%\text{--}4.06\%$ )	$-29.75\text{--}35.86$ ( $-17.92\%\text{--}21.60\%$ )
$R_{lwd} (\text{W}\cdot\text{m}^{-2})$	$-20.98\text{--}20.98$	$-2.50\text{--}2.50$ ( $-1.63\%\text{--}1.63\%$ )	$-15.54\text{--}15.54$ ( $-9.36\%\text{--}9.36\%$ )
$u (\text{m} \cdot \text{s}^{-1})$	$-1.71\text{--}1.71$	$-9.47\text{--}7.31$ ( $-6.18\%\text{--}4.77\%$ )	$9.47\text{--}7.31$ ( $5.71\%\text{--}4.41\%$ )
$T_a (\text{K})$	$-2.08\text{--}2.08$	$14.64\text{--}16.94$ ( $9.55\%\text{--}11.05\%$ )	$-14.64\text{--}16.94$ ( $-8.82\%\text{--}10.20\%$ )
SH ( $\text{kg} \cdot \text{kg}^{-1}$ )	$-0.56 \times 10^{-3} \text{--} 0.56 \times 10^{-3}$	$-0.01\text{--}0.01$ ( $-0.01\%\text{--}0.01\%$ )	$0.01\text{--}0.01$ ( $0.01\%\text{--}0.01\%$ )
$P_s (\text{hPa})$	$-8.51\text{--}8.51$	$-0.01\text{--}0.01$ ( $-0.01\%\text{--}0.01\%$ )	$0.01\text{--}0.01$ ( $0.01\%\text{--}0.01\%$ )

(2) P8-line 2-6: The introduction of the GLDAS dataset should not belong to Result. The authors should introduce it more in light of its importance for comparison.

**Author Response:** The introduction of the GLDAS dataset has been moved to section 2 (P5, L26-30). We also introduce the importance of a comparison with the GLDAS product as follows (P5, L22-26).

The high-quality, global land surface fields provided by GLDAS support weather and climate prediction, water resources applications, and water cycle investigations. Since the GLDAS data have been widely used, it is meaningful to compare our satellite estimation with these high-quality data to further prove the accuracy of our estimations.

(3) *P8-line 5: what high accuracy?*

**Author Response:** This term has been replaced with ‘high quality’. (P11, L18)

(4) *P9-line 15-27: the authors describe the feature of diurnal variation of hourly flux map.*

*Are there any special in comparison on our general understanding?*

**Author Response:** The qualitative description of diurnal variation in the hourly flux map is aligned with general knowledge. This alignment can further prove the effectiveness of our estimation method and validate the final estimation results. In the revised manuscript, we also added some quantitative expressions to improve the content. (P10)

(5) *Table 4: add values of the same indicators for all sites.*

**Author Response:** For the data quality, QA<5 was chosen to ensure the flux measurements are under similar steady state and developed conditions; thus, it is not necessary to make a comparison at each station separately. Furthermore, if we list the same indicators for all sites, two additional pages will be needed to show this content. Adding this information may make the text difficult to read. Therefore, we would like to keep the original Table 4, but the indicators for latent heat flux have been replaced by the values before the Bowen ratio correction, as you suggested.

(6) *Figure 1: the caption is too brief. The same problems for other plots. What is the right plot?*

**Author Response:** Thank you for this comment. The right plot illustrates the location of the Tibetan Plateau in China. We have improved all figure captions in the revised

manuscript. (P19-24)

(7) *Figure 4: the scale of the axis is misleading. Besides, how do you choose the representative days for each month? Choose the nice one? Please describe what they are in subpanels.*

**Author Response:** Figure 4 (now Fig. 5) has been redrawn to improve its clarity. We also added additional explanations in the figure caption to prevent ambiguity. We did not select the nice days. Instead, the monthly mean value is shown in Figure 5. The subpanels are described in the caption of the new Figure 5. (P23)

## **Response to Reviewer #2**

*This is an integral work for estimation of land surface heat fluxes based on remote sensing data, reanalysis meteorological data, and in-situ observations. The derived land surface heat flux, more like a heat flux dataset, was evaluated using observations of six eddy-covariance sites on the Tibetan Plateau (TP). And then, the diurnal and seasonal variations of the heat fluxes were also analyzed. This is of general interest for the readers of this journal. The TP is notorious for its lack of meteorological observations, which cripples the predictive power of numerical models for this region. The land surface heat fluxes are crucial for understanding energy and water cycle and also are the boundary conditions for numerical weather and climate simulations. This paper provides an integral investigation for land surface heat fluxes over the TP which will help better understanding the land-atmosphere interactions over this region. More importantly, this paper is one of the very few works to estimate land surface heat fluxes over the TP using high temporal resolution geostationary satellite data. The manuscript is well organized. Numbers of work are integrated into this paper, and abundant discussions are presented as well. I suggest acceptance after a minor revision.*

**Author Response:** We would like to thank Reviewer #2 for the positive and constructive comments. All your thoughtful comments and suggestions have been taken into account to improve our manuscript. Please find our point-by-point responses below.

(1) P1, L16: “which” → “where”.

**Author Response:** This item has been corrected. (P1, L16)

(2) P1, L18-19: Change the sentence to “However, the high temporal-resolution information about the plateau-scale land surface heat fluxes has lacked for a long time, which significantly limit the understanding of diurnal variations in land-atmosphere interactions.”

**Author Response:** Thank you for this detailed suggestion. The sentence has been revised. (P1, L18-20)

(3) P1, L20: “a” → “the”.

**Author Response:** This item has been corrected. (P1, L21)

(4) P1, L21: “*with a spatial resolution*” → “*at a spatial resolution*”.

**Author Response:** This item has been corrected. (P1, L22)

(5) P4, L9: *The sentence “These stations are the only stations currently available: : ...” is not accurate. I am quite sure that there are other eddy-covariance sites on the TP apart from the six stations mentioned in the paper.*

**Author Response:** Yes, you are correct. There are several other eddy-covariance sites on the TP. However, these sites belong to different institutes, and the data are not available to the scientific community.

(6) P7, Equation (11) and (13): “*Hs*” → “*Hs*”.

**Author Response:** These items have been corrected. (P7)

(7) P8, L4: *I do not think “Zhong et al., 2011” is a proper reference here. Perhaps you cite the paper which introduces the production of GLDAS data.*

**Author Response:** Thank you for this suggestion. Rodell et al. published a paper in BAMS in 2004 to introduce the GLDAS data. This reference has been added. (P5, L23)

(8) P8, L12: *Provide some references for “traditional polar orbiting satellite” to strengthen your argument.*

**Author Response:** Thank you for your constructive suggestion. The following references have been added. (P8, L23-24)

Ma, Y., Zhong, L., Su, Z., Ishikawa, H., Menenti, M. and Koike, T.: Determination of regional distributions and seasonal variations of land surface heat fluxes from Landsat-7 Enhanced Thematic Mapper data over the central Tibetan Plateau area, J. Geophys. Res.-Atmos., 111, D10305, DOI: 10.1029/2005JD006742, 2006.

Ma W, Ma, Y. and Ishikawa, H.: Evaluation of the SEBS for upscaling the evapotranspiration based on in-situ observations over the Tibetan Plateau, Atmos. Res., 138, 91-97, 2014.

Zou, M., Zhong, L., Ma, Y., Hu, Y., Huang, Z., Xu, K., and Feng, L.: Comparison of two satellite-based evapotranspiration models of the Nagqu River Basin of the Tibetan Plateau. *J. Geophys. Res.-Atmos.*, 123, 3961–3975, DOI: 10.1002/2017JD027965, 2018.

(9) *P10, L23*: “*land-atmosphere heat flux data*” → “*land surface heat flux data*”.

**Author Response:** This item has been corrected.(P11, L14)

(10) *P10, L24*: Delete “*using a combination of geostationary and polar orbiting satellite data*”.

**Author Response:** This phrase has been deleted.

(11) *The English need substantial improvement. Please find a native speaker to help you to polish the manuscript.*

**Author Response:** According to your suggestion, the revised manuscript has been edited by a native English speaker.

## **Response to Reviewer #4**

*High temporal resolution surface heat fluxes are very important for land-atmosphere interactions. In this manuscript, land surface temperature from polar and geostationary satellite are both used and fed into surface energy balance equation. The results are validated with flux tower observations, and finally hourly surface heat fluxes with 5 km spatial resolution are generated over TP based on the developed SEB scheme. Generally, the manuscript is interesting and well written. It can be published with minor revisions.*

**Author Response:** We would like to sincerely thank the reviewer for the thoughtful comments and suggestions. Please see our responses to your comments and suggestions below.

(1) *Page 2, Line 30: I think the authors missed an important kind of method (data assimilation method) for surface heat flux estimations based on remotely sensed LST. Some reference are as follows,*

*Abdolghafoorian, A., Farhadi, L., Bateni, S.M., Margulis, S., Xu, T.R. (2017). Characterizing the effect of vegetation dynamics on the bulk heat transfer coefficient to improve variational estimation of surface turbulent fluxes. J. Hydrometeorol. 18, 321–333.*

*Bateni, S.M., Entekhabi, D., & Castelli, F. (2013). Mapping evaporation and estimation of surface control of evaporation using remotely sensed land surface temperature from a constellation of satellites, Water Resour. Res., 49, 950-968, doi:10.1002/wrcr.20071.*

*Crow, W.T., & Kustas, W.P. (2005). Utility of assimilating surface radiometric temperature observations for evaporative fraction and heat transfer coefficient retrieval, Bound-Lay. Meteorol., 115(1), 105-130, doi:10.1007/s10546-004-2121-0.*

*Xu, T, Bateni, S.M., Liang, S., Entekhabi, D., & Mao, K. (2014). Estimation of surface turbulent heat fluxes via variational assimilation of sequences of land surface temperatures from Geostationary Operational Environmental Satellites, J. Geophys. Res., 119, 10,780-10,798, doi:10.1002/2014JD021814.*

*Xu, T.R., He, X.L., Bateni, S.M., Auligne, T., Liu, S.M., Xu, Z.W., Zhou, J., Mao, K.B.(2019). Mapping Regional Turbulent Heat Fluxes via Variational*

*Assimilation of Land Surface Temperature Data from Polar Orbiting Satellites, Remote Sensing of Environment, 221, 444-461, <https://doi.org/10.1016/j.rse.2018.11.023>.*

**Author Response:** Thank you for your helpful suggestion. We totally agree with you. Land surface temperature and vegetation information from satellites have been used to estimate regional land surface heat fluxes by different assimilation techniques in recent years. All the above references together with the following comments have been added to the revised manuscript. (P3, L9-15)

In recent years, land surface temperature and vegetation index data retrieved from satellites have been successfully assimilated in the variational data assimilation (VDA) frameworks to estimate surface heat fluxes (Crow and Kustas 2005; Bateni et al., 2013; Xu et al., 2014; Abdolghafoorian et al., 2017; Xu et al., 2019). This kind of method does not require any empirical or site-specific relationships and can provide temporally continuous surface heat flux estimates from discrete spaceborne land surface temperature (LST) observations (Xu et al., 2014).

(2) *How to derive 5 km and hourly surface heat fluxes with 10 km and 3 hour forcing data?*

**Author Response:** The final resolution of our product should be determined by the lowest resolution of the source data. Thus, the final surface heat flux product should be 10 km. We corrected this mistake in the manuscript after the quick review by one of the reviewers.

It should also be noted that the forcing dataset of ITPCAS has a spatial resolution of 10 km and a temporal resolution of 3 hours. For the temporal resolution, a linear statistical downscaling method was used to derive hourly meteorological forcing data based on the original 3-hour forcing data and in situ measurements in this study. The general idea is to establish an empirical relationship between each 3-hour measurement. Then, this relationship is applied to meteorological forcing data (P5, L17-21). For example,  $T_{a00}$ ,  $T_{a01}$  and  $T_{a03}$  represent the in situ air temperature measurements from six stations at 00 h, 01 h and 03 h, respectively. Thus,  $T_{a00} = [a_1, a_2, a_3, a_4, a_5, a_6]$ ,  $T_{a01} = [b_1, b_2, b_3, b_4, b_5, b_6]$ , and  $T_{a03} = [c_1, c_2, c_3, c_4, c_5, c_6]$ . Then, the linear equation  $T_{a01} = k_1 T_{a00} + k_2 T_{a03}$  can be solved. According to the meteorological forcing data at 00h and 03h, the plateau scale  $T_a$  at 01h can be

achieved by the following formula.

$$\begin{pmatrix} b_{11} & \cdots & b_{1n} \\ \vdots & \ddots & \vdots \\ b_{m1} & \cdots & b_{mn} \end{pmatrix} = k_1 \begin{pmatrix} a_{11} & \cdots & a_{1n} \\ \vdots & \ddots & \vdots \\ a_{m1} & \cdots & a_{mn} \end{pmatrix} + k_2 \begin{pmatrix} c_{11} & \cdots & c_{1n} \\ \vdots & \ddots & \vdots \\ c_{m1} & \cdots & c_{mn} \end{pmatrix}$$

where  $a$ ,  $b$  and  $c$  represent meteorological forcing data at 00 h, 01 h and 03 h, respectively; and  $m$  and  $n$  represent total rows and columns, respectively, of the grid data. The meteorological forcing data at other times can be similarly determined.

(3) In equation 5, sensible heat flux is represented as  $H_s$ , while it is  $H$  in equation 11.

*They should be the same in one manuscript.*

**Author Response:** This item has been corrected to keep the same format. (P7)

(4) What is the time period of this study? as well as validation results in Table 3.

**Author Response:** The time period for all meteorological data and satellite data covers the whole year of 2008. This information has been added in section 2. (P5, L9-10)

(5) Figure2: the 'ITPCAS' is a name of institute, not data. It should be changed into 'Meteorological data' or something else.

**Author Response:** 'ITPCAS' in Figure 2 has been replaced with 'Meteorological forcing data'. (P20)

(6) Figure 3: the estimated  $G_0$  has a big bias against ground measurements. This is because  $G_0$  is parameterized with  $R_n$ .  $G_0$  and  $R_n$  do not have the same diurnal variation shape. The  $G_0$  peak values are usually later than  $R_n$ . However, the parameterization did not consider this. The authors may discuss this in the manuscript.

**Author Response:** Thank you for this insightful comment. We discuss the large bias in estimated soil heat flux as follows. (P8, L7-12)

It should be noted that some bias exists between the estimated soil heat flux and ground measurements because soil heat flux is parameterized with net radiation flux (equation (8)). However, soil heat flux and net radiation flux do not have the same diurnal variation shape. The soil heat flux peak values are usually later than the net radiation flux peak values, which was not taken into account in the parameterization.

Thus, development of a better parameterization scheme for soil heat flux is needed.

(7) *Figure 4: usually, the observations were drawn by open cycles, and estimations are drawn by solid lines.*

**Author Response:** Figure 4 (now Figure 5) has been redrawn according to your suggestion. (P23)

(8) *Why  $R_n$  is underestimated from June to Aug. at BJ site in figure 4? Why  $H$  (LE) is underestimated (overestimated) from Jan. to May? The authors should give some explanations.*

**Author Response:** As shown by the surface radiation balance equation (equation (6)), the downward short radiation is the main incoming energy. A comparison was made between the forcing data and in situ downward radiation at BJ station. From June to August, the monthly diurnal MB was  $-4.87 \text{ Wm}^{-2}$ , which explains why the derived net radiation flux was underestimated by the SEBS model from June to August. This phenomenon was also found in the study by Yang et al. (2010). As for the time period from January to May, the underestimation of sensible heat flux was mainly caused by the negative bias of the land-atmosphere air temperature difference. The MB for the land-atmosphere difference could be  $-5.69 \text{ K}$  from January to May. As there is a complementary relationship between sensible heat flux and latent heat flux, the corresponding latent heat flux tends to be overestimated. This discussion has been added to the revised manuscript. (P10, L8-18)

(9) *Figure 5: the authors give two days of diurnal cycles over TP. The results are from which day and which year? It should be noted on figure 5. In addition, why you choose these two days?*

**Author Response:** It should be noted here that the diurnal cycles of land surface heat flux are based on the annual mean of 2008. The top panels are sensible heat flux, and the bottom panels are latent heat flux. We have added this information in the figure caption. (P24)

# Estimation of Hourly Land Surface Heat Fluxes over the Tibetan Plateau by the Combined Use of Geostationary and Polar Orbiting Satellites

Lei Zhong<sup>1</sup>, Yaoming Ma<sup>2,3,4</sup>, Zeyong Hu<sup>3,5</sup>, Yunfei Fu<sup>1</sup>, Yuanyuan Hu<sup>1</sup>, Xian Wang<sup>1</sup>,

5 Meilin Cheng<sup>1</sup>, Nan Ge<sup>1</sup>

<sup>1</sup>School of Earth and Space Sciences, University of Science and Technology of China, Hefei 230026, China

<sup>2</sup>Key Laboratory of Tibetan Environment Changes and Land Surface Processes, Institute of Tibetan Plateau Research, the Chinese Academy of Sciences, Beijing 100101, China

10 <sup>3</sup>CAS Center for Excellence in Tibetan Plateau Earth Sciences, Beijing 100101, China

<sup>4</sup> University of Chinese Academy of Sciences, Beijing 100049, China

<sup>5</sup> Northwest Institute of Eco-Envrionment and Resources, the Chinese Academy of Sciences, Lanzhou 730000, China

*Correspondence to:* Lei Zhong ([zhonglei@ustc.edu.cn](mailto:zhonglei@ustc.edu.cn))

15 **Abstract.** ~~The estimation of land surface heat fluxes has significant meaning is important~~ for energy and water cycle studies, especially ~~for on~~ the Tibetan Plateau (TP), ~~whichwhere has unique the~~ topography ~~is unique~~ and ~~the strong~~ land-atmosphere interactions ~~are strong~~. The land surface heating ~~status conditions~~ also directly influences the movement of atmospheric circulation. ~~However, high temporal resolution information on the plateau-scale land surface heat fluxes has lacked for a long time,~~ which significantly limits the understanding of diurnal variations in land-atmosphere interactions. ~~However, for a long time, plateau scale land surface heat flux information with high temporal resolution has been lacking, which greatly limits understanding of diurnal variations in land-atmosphere interactions.~~ Based on geostationary and polar orbiting satellite data, ~~a the~~ surface energy balance system (SEBS) was used in this paper to derive hourly land surface heat fluxes ~~with at~~ a spatial resolution of 10 km. Six stations scattered ~~throughout~~ the TP and equipped for flux tower measurements were used to ~~correct the energy imbalance problem existing in the measurements and to~~ perform ~~a~~ cross-validation. The results showed good agreement between ~~the~~ derived fluxes and in situ measurements through 3738 validation samples. The ~~root mean square errors~~ (RMSEs) for net radiation flux, sensible heat flux, latent heat flux and soil heat flux were  $76.63 \text{ Wm}^{-2}$ ,  $60.29 \text{ Wm}^{-2}$ , ~~71.03~~  $\text{Wm}^{-2}$  and  $37.5 \text{ Wm}^{-2}$ , respectively. The derived results were also found to be superior to ~~the~~ GLDAS flux products (~~with~~ RMSEs for the surface energy balance components ~~were of~~  $114.32 \text{ Wm}^{-2}$ ,  $67.77 \text{ Wm}^{-2}$ ,

20

25

30

75.6 Wm<sup>-2</sup> and 40.05 Wm<sup>-2</sup>, respectively). The diurnal and seasonal cycles of land surface energy balance components were clearly identified and. Their spatial distribution was found to be consistent with the heterogeneous land surface conditions and the general hydrometeorological conditions of the TP.

## 5 1. Introduction

Mass and energy exchanges are constantly carried out between the land surface and the atmosphere above. At the same time, the weather, climate and environmental changes at multiple spatiotemporal scales are greatly influenced by such land-atmosphere exchanges. Land-atmosphere interaction is a popular topic not only in the field of atmospheric research but also in hydrology, 10 geography, ecology and environmental sciences (Ye and Fu 1994). The impacts of land-atmosphere interactions on weather and climate change have been assessed through surface sensible heat flux, latent heat flux and momentum flux (Seneviratne et al, 2008; Ma et al, 2017). How Developing a method to accurately derive the surface heat fluxes has always been a main research question and a primary focus of in atmospheric science research.

15 The Tibetan Plateau (TP), with an average elevation of more than 4000 m, is also called ‘the Third Pole’ and ‘the World Roof’. The thermal and dynamic effects caused by the TP’s high elevation and relief have profound impacts on atmospheric circulation, the Asian monsoon and global climate change (Ye and Gao 1979; Ma et al, 2006; Ma et al, 2008; Zhong et al, 2011; Zou et al, 2017; Zou et al, 2018).

20 The interactions between TP multispheres, such as the atmosphere, hydrosphere, lithosphere, biosphere, and cryosphere, are the drivers of all these changes. The TP is also one of the most sensitive regions in response to global climate change (Liu et al, 2000). In recent years, some studies have argued that the major factor impacting the South Asian monsoon is the insulating effect of the southern mountain edges

25 of the Tibetan Plateau TP, rather than the elevated heating by the Tibetan Plateau TP (Boos and Kuang 2010; Boos and Kuang 2013). However, some other studies have proven that the thermal effects of the

25 TP are the main driving force of the South Asian summer monsoon (Wu et al, 2012; Wu et al, 2015).

Obviously, opinions differ in understanding the thermal forcing by the TP. One of the most important reasons is that high spatial and temporal resolution data on land-atmosphere interactions, which can be used in different climate models, are still lacking. To study the characteristics of land-atmosphere interactions in the TP, it is necessary to estimate the surface energy heat fluxes with a fine spatial and

30 temporal resolution over the TP.

Traditional surface energy flux measurements are not only expensive but also limited at the point scale. It and it is impossible to meet the need for a larger spatial scale with the complex terrain and landscapes of the TP. However, Remote sensing provides the possibility of deriving surface heat fluxes at a regional scale (Ma et al, 2002; Zhong et al, 2014). The methods of estimating surface energy flux by remote sensing can be roughly divided into two-three categories: the empirical (semiempirical) model-and-theoretical model-and data assimilation system. The empirical (semiempirical) model is mainly based on an empirical formula between surface energy fluxes and surface characteristic parameters. The method itself is simple, but its applicability is limited. The basis of the theoretical model is the surface energy balance equation. The physical model mainly includes a single source model and a double source model. The single source model does not distinguish vegetation transpiration and soil evaporation but tends to consider them as a whole (Su, 2002; Jia et al., 2003; Roerink et al., 2000; Bastiaanssen et al., 1998; Allen et al., 2007). The double source model separates the vegetation canopy from the soil and calculates the soil temperature and canopy temperature. Then, the sensible heat flux and latent heat flux are also calculated (Norman et al, 1995; Sánchez et al, 2008). In recent years, the land surface temperature and vegetation index data retrieved from satellite have been successfully assimilated in the variational data assimilation (VDA) frameworks to estimate surface heat fluxes (Crow and Kustas 2005; Bateni et al., 2013; Xu et al., 2014; Abdolghafoorian et al., 2017; Xu et al., 2019). This kind of method does not require any empirical or site-specific relationships and can provide temporally continuous surface heat flux estimates from discrete spaceborne land surface temperature (LST) –observations (Xu et al., 2014).

Some studies have been carried out to estimate surface energy fluxes over the TP based on polar orbiting satellite data. Ma et al. (2003) estimated the surface energy flux of the CAMP (CEOP Asia–Australia monsoon project)/Tibet area using NOAA-14/AVHRR data. The results show that the estimated surface energy flux is in good agreement with the in situ measurements. Oku et al. (2007) used land surface temperature LST derived from the Geostationary Meteorological Satellite (GMS)-5 and other essential parameters from NOAA-AVHRR, ERA-40 to estimate land surface heat fluxes for regions above 4000 m over the TP. However, the coarse resolution of EAR-40 (25 km) and large error of LST (more than 10 K) brought introduced large uncertainties into the final results. Ma et al. (2009) estimated the surface characteristic parameters and surface energy flux of the northern Tibetan Plateau TP in summer, winter and spring using a parameterized scheme for ASTER satellite data. Chen

et al. (2013a) used observations from 4 sites in the TP to evaluate the results of the [surface energy balance system](#) (SEBS) model and optimize the thermodynamic roughness parameterization scheme for [the](#) underlying surface of bare soil. Based on Landsat TM/ETM+ data, Chen et al. (2013b) derived the surface energy flux of the Mount Everest area by using the enhanced SEBS model (TESEBS), which [takes takes into account](#) the influence of terrain factors on [the](#) solar radiation [into account](#), and the SEBS model. The results show that the estimated results from the TESEBS model are superior to those from the SEBS model [for high resolution satellite images](#).

At present, the estimation of the surface energy flux of the TP is mainly based on polar orbit satellite data. Because of the low temporal resolution of the polar orbit satellites, time series of land-atmosphere energy and water exchange data with high temporal resolution in the TP have not been retrieved to date, and the effective basic parameters for the climate model cannot yet be provided. In addition, one of the basic characteristics of the atmospheric boundary layer is its diurnal variation, and information on daily variations in surface energy flux is also lacking over the TP. [Furthermore, in previous studies of surface energy flux estimation, the accuracy of the model estimation is usually validated directly by the in situ measurements. The "energy closure" problem existing in the surface flux observation data has not received much attention, and the validation results have some uncertainties. Many previous studies have shown that there is a widespread "energy unclosed" problem in surface flux observations \(Twine et al, 2000; Lee et al, 2002; Mauder et al, 2007; Yang et al, 2008\).](#) Pan et al. (2017) noted that the latent heat flux can be significantly underestimated by the eddy correlation method, while the Bowen ratio correlation method, which is based on the surface energy balance equation and the gradient diffusion theory of the surface layer, can effectively improve the underestimation of the latent heat flux.

This paper mainly focused on how to acquire time series of energy flux data with high temporal resolution using a combination of geostationary and polar orbiting satellite data. First, [based on the surface flux measurements in the TP, the problem of "energy closure" in the observational data was improved by using the Bowen ratio calibration method. Then](#), the surface energy fluxes over the TP were estimated using the SEBS model with inputs from high temporal resolution [land surface temperature](#) LST from FY-2C data and other land surface characteristic parameters from polar orbiting satellite data. [Then](#) the derived land surface heat fluxes were validated by flux tower measurements and were also compared with [Global Land Data Assimilation System \(GLDAS\)](#) flux products. The study

area and datasets used in this study are introduced in section 2. The model description is given in section 3, followed by the results and discussion in section 4. The main conclusions are drawn in section 5.

## 5      2. Study Area and Data

The TP, located in southwest China, has an area of approximately  $2.5 \times 10^6$  km<sup>2</sup> (Fig. 1) ~~and~~It is the largest plateau in China. With an average elevation of approximately 4000 m, ~~it is the TP~~ also the highest plateau in the world, and the high elevation can directly influence the middle and upper layers of the atmosphere. ~~For a long time,~~ ~~Due~~ Due to the harsh climate conditions and complex topography of the TP, ~~the~~ meteorological stations in this area ~~have been rare~~ not only sparse but also unevenly ~~distributed~~. A total of 6 meteorological stations ~~are have been~~ used ~~to compare for comparison~~ with model estimates. Although these 6 ~~station sites~~ are not scattered throughout the entire TP, they include several major land cover types (Zhong et al, 2010), and their elevation varies from 3000 m to 5000 m (Table 1). These stations are the only stations currently available, and each station is equipped to make four-component radiation measurements, soil moisture and temperature measurements, eddy-covariance measurements and conventional observation items such as wind speed ( $u$ ), air temperature ( $T_a$ ), specific humidity (SH) and air pressure ( $P_s$ ). 

Both the geostationary satellite Feng Yun 2C (FY-2C) and the polar orbiting satellite SPOT are used to retrieve the essential land surface characteristic parameters. The stretched visible and infrared spin scan radiometer (SVISSR) onboard FY-2C is used to derive the hourly ~~land surface temperature~~ ~~LST~~ with a spatial resolution of 5 km following the algorithms developed by our group (Hu et al, 2018). We should point out here ~~is~~ that SVISSR has no infrared channel, which would be needed to derive normalized difference vegetation index (NDVI), albedo and emissivity. ~~Suppose that~~If these parameters (NDVI, albedo and emissivity) have little variation during a day; then, the product of the orbiting satellite SPOT is used instead. The spatial resolution for NDVI, albedo and emissivity is 1 km with a daily temporal resolution. All the above satellite data with a higher spatial resolution were resampled to match the resolution of the meteorological forcing data (Zou et al, 2018). The time period for all meteorological data and satellite data covers the whole year of 2008.

A forcing dataset developed by the Institute of Tibetan Plateau Research, Chinese Academy of Sciences (ITPCAS), is used as ~~the~~ model input in this study. The dataset has merged the observations

from 740 operational stations of the [China Meteorological Administration \(CMA\)](#) with the corresponding Princeton global meteorological forcing dataset (He, 2010; Yang et al, 2010). The parameters used in this study are downward shortwave radiation ( $R_{swd}$ ), downward longwave radiation ( $R_{lwd}$ ), wind speed, air temperature, specific humidity and air pressure. All these parameters have a spatial resolution of 10 km and a temporal resolution of 3 hours (Table 2). [A linear statistical downscaling method was used to derive hourly meteorological forcing data based on original 3-hour forcing data and in situ measurements in this study. The general idea is to establish an empirical relationship between each 3-hour measurements. Then this relationship will be applied to the meteorological forcing data.](#)

[The Global Land Data Assimilation System \(GLDAS\) products are produced by combining satellite and ground-based observations using advanced land surface modeling and data assimilation techniques \(Rodell et al, 2004; Zhong et al, 2011\). These products have been proved to simulate optimal fields of land surface states and fluxes in near-real time \(Rodell et al, 2004\). Here, 3-hour land surface heat flux products with a spatial resolution of 25 km are selected for comparison with satellite estimates.](#)

Since 6 stations in Table 1 were not used in [the ITPCAS meteorological](#) forcing data, they can be used as independent data to validate the accuracy of [the](#) forcing meteorological data. The [RMSE](#) (root mean square error [\(RMSE\)](#)), [MB](#) (mean bias [\(MB\)](#)), [MAE](#) (mean absolute error [\(MAE\)](#)) and [R](#) (correlation coefficient [\(R\)](#)) are used to make a comparison between [the](#) ITPCAS forcing data and in situ meteorological data.

$$RMSE = \sqrt{\frac{\sum_{i=1}^N (x_i - obs_i)^2}{N}} \quad (1)$$

$$MB = \frac{\sum_{i=1}^N (x_i - obs_i)}{N} \quad (2)$$

$$MAE = \frac{\sum_{i=1}^N |x_i - obs_i|}{N} \quad (3)$$

$$R = \frac{\sum_{i=1}^N (x_i - \bar{x})(obs_i - \bar{obs})}{\sqrt{\sum_{i=1}^N (x_i - \bar{x})^2} \sqrt{\sum_{i=1}^N (obs_i - \bar{obs})^2}} \quad (4)$$

where  $x_i$  and  $obs_i$  are [the](#) estimation and measurement, respectively.  $\bar{x}$  and  $\bar{obs}$  are the average values of [the](#) estimation and measurement, respectively. As [seen from shown in](#) Table 3, all six parameters show reasonable accuracy with [the](#) in situ measurements, which means these forcing parameters can be used as model inputs.

### 3. Model Description

Fig. 2 shows the general steps to derive the land surface heat fluxes in this paper. The SEBS model is used in this study. Because the surface energy balance has the four components of radiation ( $R_n$ ), sensible heat flux ( $H_s$ ), latent heat flux (LE) and soil heat flux ( $G_0$ ), the energy balance equation can be written as

$$R_n = H_s + LE + G_0 \quad (5)$$

where  $R_n$  can be determined by the surface radiation equation as

$$R_n = R_{swd}(1 - \alpha) + \varepsilon_a \sigma T_a^4 - \varepsilon_s \sigma T_s^4 \quad (6)$$

where  $R_{swd}$  is the downwelling solar radiation at the land surface. Because there are no infrared channels on board FY-2C, the NDVI,  $\alpha$  and  $\varepsilon_s$  are derived from SPOT/VGT data.  $\alpha$  is the broadband albedo, which can be derived from the narrowband reflectance of VGT  $\alpha_1, \alpha_2, \alpha_3$  and  $\alpha_4$  (Zou et al, 2018).  $\alpha_1, \alpha_2, \alpha_3$  and  $\alpha_4$  refer to the reflectance of the blue band, red band, near infrared band and short wave infrared band, respectively.

$$\alpha = -0.8141\alpha_1 + 0.4254\alpha_2 + 1.2605\alpha_3 - 0.2902\alpha_4 + 0.1819 \quad (7)$$

The  $\sigma$  in equation (6) is the Stefan-Boltzmann constant ( $5.76 \times 10^{-8} \text{ W}\cdot\text{m}^{-2}\cdot\text{K}^{-4}$ ).  $\varepsilon_a$  and  $\varepsilon_s$  are the emissivities of surface air and the land surface, respectively.  $T_a$  and  $T_s$  are the surface air temperature and land surface temperature LST, respectively. The hourly  $T_s$  is derived from split window algorithms (Hu et al, 2018) based on two thermal bands of FY-2C.

The soil heat flux is determined by net radiation flux and vegetation coverage.

$$G_0 = R_n[\Gamma_c + (1 - f_c)(\Gamma_s - \Gamma_c)] \quad (8)$$

where  $\Gamma_s$  and  $\Gamma_c$  are ratios of soil heat flux and net radiation flux for bare soil and full vegetation cover, respectively.  $f_c$  is vegetation coverage and can be derived from NDVI as follows.

$$f_c = \left( \frac{NDVI - NDVI_{min}}{NDVI_{max} - NDVI_{min}} \right)^2 \#(9)$$

$$NDVI = \frac{\alpha_3 - \alpha_2}{\alpha_3 + \alpha_2} \#(10)$$

By using the wind speed and air temperature at the reference height, the sensible heat flux, together with the friction velocity and Obukhov stability length, can be derived by solving the following nonlinear equations (11-13). Then, the latent heat flux can be estimated by applying equation (5).

$$L = -\frac{\rho \cdot c_p \cdot \theta_v \cdot u_*^3}{k \cdot g \cdot H_s H_s} \#(11)$$

$$u_* = k \cdot u \cdot \left[ \ln \left( \frac{z - d_0}{z_{0m}} \right) - \Psi_m \left( \frac{z - d_0}{L} \right) + \Psi_m \left( \frac{z_{0m}}{L} \right) \right]^{-1} \#(12)$$

$$H_s H_s = k \cdot u_* \cdot \rho \cdot c_p \cdot (\theta_0 - \theta_a) \cdot \left[ \ln \left( \frac{z - d_0}{z_{0h}} \right) - \Psi_h \left( \frac{z - d_0}{L} \right) + \Psi_h \left( \frac{z_{0h}}{L} \right) \right]^{-1} \#(13)$$

where L is the Obukhov length,  $c_p$  is the specific heat at constant pressure,  $\theta_v$  is the surface potential virtual air temperature,  $u_*$  is the friction velocity,  $k = 0.4$  is the von Karman constant, g is the acceleration due to gravity,  $H_s$  is the sensible heat flux,  $u$  is the mean wind speed at reference height z,  $d_0$  is the zero plane displacement height,  $z_{0m}$  is the roughness height for momentum transfer,  $z_{0h}$  is the roughness height for heat transfer,  $\Psi_m$  is the stability correction function for momentum heat transfer,  $\Psi_h$  is the stability correction function for sensible heat transfer and  $\theta_0$  and  $\theta_a$  are the potential temperatures at the surface and reference height, respectively.

#### 4. Results and Discussion

##### 10 4.1 Validation Against In Situ Flux Tower Measurements

With the aid of SPOT/VGT and FY-2C/SVISSR data, the surface energy budget components have been estimated using the SEBS model. The accuracy of these estimates needs to be validated before further analyses. A total of 6 stations over the TP equipped with eddy-covariance measurements were selected for validation (Table 1). These validation stations cover a variety of climates, land cover types and elevations.

The in-situ flux data have been flagged by steady state tests and developed conditions tests according to Foken and Wichura (1996) and Foken et al. (2004). The steady conditions means that all statistical parameters do not vary within time. The flux-variance similarity was used to test the development of turbulent conditions. Only the A data quality of only QA<5 was chosen to make the comparison. The ‘energy imbalance’ is an important research issue and has been widely reported in former studies (Twine et al., 2000; Wilson et al., 2002; Wolf et al., 2008; Majozi et al., 2017; Pan et al., 2017). If these measurements were not corrected and directly used to compare with estimates, some discrepancies would appear. Therefore, a so-called Bowen ratio correction method (Twine et al., 2000; Wilson et al., 2002; Hu et al., 2018) is used to process the in-situ flux measurements. The results show that the energy closure ratio can be improved by approximately 20% for different stations (Hu et al., 2018). Then, the corrected in-situ flux measurements are used to validate the satellite estimates. As shown in Fig. 3a, 3b, 3c and 3d, the estimates of surface energy budget components show reasonable

agreement with the in situ measurements. The RMSEs for the net radiation flux, sensible heat flux, latent heat flux and soil heat flux are  $76.63 \text{ Wm}^{-2}$ ,  $60.29 \text{ Wm}^{-2}$ ,  $71.03 \text{ Wm}^{-2}$  and  $37.5 \text{ Wm}^{-2}$ , respectively. The total validation numbers (N) are more than 3837 to make the results much more representative and convincing. It should be noted that some bias exists between the estimated soil heat flux and ground measurements. This is because soil heat flux is parameterized with net radiation flux (Equation (8)). However, soil heat flux and net radiation flux do not have the same diurnal variation shape. The soil heat flux peak values are usually later than the net radiation flux peak values, which was not taken into account in the. The parameterization did not take this into account. Thus, development of a How to better parameterization scheme fore the soil heat flux remains an open issue is needed.

The high-quality, global land surface fields provided by GLDAS support weather and climate prediction, water resources applications, and water cycle investigations. Since the GLDAS data have been widely used, it is meaningful to make a comparison compare our satellite estimations with these high-quality data to further prove the accuracy of our satellite estimations. To test the robustness of our results, the surface energy budgets obtained from the Global Land Data Assimilation System (GLDAS) data are selected for comparison with the FY-2C estimations. The GLDAS products are produced by combining satellite and ground based observations using advanced land surface modeling and data assimilation techniques (Zhong et al., 2011). These products have been proved to simulate key variables and fluxes with high accuracy (Rodell et al., 2004). Here, 3 hour land surface heat flux products with a spatial resolution of 25 km are selected for comparison with satellite estimates. The comparison shows that the accuracies of the surface energy budgets from the satellite estimation are much higher than those of the GLDAS products (Table 44). The RMSE of the net radiation flux is reduced from  $114.32 \text{ Wm}^{-2}$  to  $76.63 \text{ Wm}^{-2}$ , while the values for sensible heat flux, latent heat flux and soil heat flux are reduced from  $67.77 \text{ Wm}^{-2}$ ,  $75.6 \text{ Wm}^{-2}$  and  $40.05 \text{ Wm}^{-2}$  to  $60.29 \text{ Wm}^{-2}$ ,  $71.03 \text{ Wm}^{-2}$  and  $37.5 \text{ Wm}^{-2}$ , respectively. Therefore, the new energy budget products not only have a finer spatial (10 km) and temporal resolution (hourly) than traditional polar orbiting satellite retrievals (e.g. Ma et al. 2006; Ma et al. 2014; Zou et al. 2018) but also possess much higher accuracy than the data assimilation results from GLDAS. Although the SEBS algorithm was used in this study and in Oku et al. (2007) (Oku 07 hereinafter), the methods to for deriving derive the land surface characteristic parameters, such as land surface temperatureLST and albedo are different (Hu et al., 2018; Oku and Ishikawa 2004; Zou et al.,

2018). The higher accuracy and finer spatiotemporal resolution of input forcing data (10km, 3 hour) and land surface characteristic parameters derived from satellites make our results more superior than those of Oku 07. It should also be noted that there is only one station used to do-perform the validation in Oku 07 while six stations with four major land cover types were used in this study to make the results much more robust. Moreover, our results cover the entire TP while Oku 07 only cover the region above 4000 m in the TP.

However, that there are indeed some discrepancies for this new product should be pointed out here, which means some room is still availableimprovements are still needed for the to improve current products. The error sources may come from multiple aspects, such as the uncertainties of input forcing data, the accuracy of land surface parameters from satellite retrievals and some assumptions and simplification in the SEBS model itself. As shown in Fig. 4, three sites located in the northern, western and southeastern parts of the TP were randomly selected to performdo the sensitivity analysis. All input meteorological forcing parameters in Table 3 ( $R_{swd}$ ,  $R_{lwd}$ ,  $u$ ,  $T_a$ , SH,  $P_s$ ) are selected. The original sensible heat flux and latent heat flux from the SEBS model are used as reference values. The RMSEs of different forcing data were used as perturbations. As shown in Table 5, the sensible heat flux is highly sensitive to  $R_{swd}$ ,  $u$  and  $T_a$ , while the latent heat flux is very sensitive to  $R_{swd}$ ,  $R_{lwd}$  and  $T_a$ . Both sensible heat flux and latent heat flux are not sensitive to errors of SH and  $P_s$ . As the  $R_{swd}$  has a variation varies from  $-68.5 \text{ Wm}^{-2}$  to  $68.5 \text{ Wm}^{-2}$ , the induced latent heat flux uncertainty ranges from  $-29.75 \text{ Wm}^{-2}$  to  $35.86 \text{ Wm}^{-2}$ . Similarly, the sensible heat flux is muchvery sensitive to  $T_a$ . When the  $T_a$  has an uncertainty from  $-2.08 \text{ K}$  to  $2.08 \text{ K}$ , the induced sensible heat flux uncertainty ranges from  $14.64 \text{ Wm}^{-2}$  to  $-16.94 \text{ Wm}^{-2}$ . Furthermore, the mismatch between in situ measurements at the point level and the scales at the pixel level or grid level may also cause some errors. The scale problem is an important research issue and should be accounted for. However, itthis issue goes beyond the scope of this study.

## 25 4.2 Multitemporal and SpatialSpatial distributionDistribution of surface Surface energy Energy budget BudgetComponentsComponents

One-year observation data and satellite estimations at BJ station were selected for comparison. As shown in Fig. 45, the satellite results can reproduce both the diurnal and seasonal surface flux variations very well. At the daily temporal scale, all the surface heat fluxes increase with sunrise and reach their maximum at mid-day before decreasing again with sunset. A unique characteristic of the

atmospheric boundary layer is its well-known diurnal variations. The diurnal pattern of derived surface heat fluxes is in agreement with the diurnal evolution of the surface atmospheric boundary layer because the surface energy budgets provide a driving force for the surface atmospheric boundary layer.

Fig. 4-5 also shows that the flux values are usually positive during the day while they and become negative in during the night. This feature means that the dynamic and thermal contrasts of land and atmosphere are totally different between day and night. The daytime surface heat fluxes during the day are much larger than the values those during the at night. At the seasonal scale, the diurnal mean net radiation flux usually increases from January (15.88 W·m<sup>-2</sup>) to its maximum in June (129.93 W·m<sup>-2</sup>). Then, it decreases again from June to December (2.07 W·m<sup>-2</sup>). The variation trends for sensible heat flux and latent heat flux are quite opposite. Because the TP is greatly influenced by the Asian monsoon system and the vegetation intensity usually increases from May to September (Zhong et al, 2010), the sensible heat flux usually decreases while the latent heat flux usually increases from the premonsoon season to the monsoon season. However, from the monsoon season to the postmonsoon season, the sensible heat flux increases while the latent heat flux decreases. The largest daily average intensity of sensible heat flux was found in April (34.97 W·m<sup>-2</sup>) while that for latent heat flux was found in June (69.09 W·m<sup>-2</sup>). As shown by the surface radiation balance equation (Equation (6)), the downward shortwave radiation is the main incoming energy. A comparison was made between the forcing data and in situ downward radiation at BJ station. From June to August, the monthly diurnal mean bias MB was -4.87 Wm<sup>-2</sup>, which explains why the derived net radiation flux was underestimated by the SEBS model from June to August. . And this phenomenon was also found in the study of by Yang et al. (2010). As for the time period from January to May, the underestimation of sensible heat flux was mainly caused by the negative bias of the land-atmosphere air temperature difference. The mean bias MB for the land-atmosphere difference could be -5.69 K from January to May. As there is a complementary relationship between sensible heat flux and latent heat flux, the corresponding latent heat flux tends to be overestimated.

A clear diurnal variation in hourly sensible heat flux and latent heat flux maps over the entire TP is shown in Fig. 56. Similar to the diurnal variations of in net radiation flux, the amplitude of the sensible heat flux is relatively small before sunrise. Then, the sensible heat flux increases quickly until it reaches its maximum at approximately 14:00 (local standard time). After this time, sensible heat flux # decreases gradually and tends to be smooth at night. The spatial distribution of sensible heat flux is

somewhat complicated. In general, because of the sparse vegetation coverage and limited soil moisture in the western TP, the sensible heat flux is much lower than that~~ese~~ in other parts of the TP. The latent heat flux tends to be zero before sunrise. With more solar energy after sunrise and much more evaporation from the soil and transpiration of vegetation, the latent heat flux rises gradually and reaches its maximum at 14:00. The spatial distribution of latent heat flux is in good agreement~~correlates well~~ with the land surface status~~conditions~~. In the southeastern part of the TP, the climate conditions are warm and wet. Thus, the vegetation density is much higher than that in the northwestern part. From southeast to northwest, the vegetation changes from forest, meadow, and grassland to sands and gravels, and the latent heat flux decreases accordingly.

10

## 5. Conclusions and remarks~~Remarks~~

A typical characteristic of the atmospheric boundary layer is diurnal variation. For a long time, little knowledge~~Limited information~~ has been acquired to understand plateau-scale land-atmosphere interactions, especially their energy and water transfers, because of the limitation of point-scale observation and the low temporal resolution of polar orbiting satellites. In this study, polar orbiting satellite data were used to retrieve land surface characteristic parameters such as NDVI, vegetation coverage, albedo and emissivity. These parameters can be considered to have relatively very small diurnal variation but large seasonal variation. For other parameters with more typical diurnal variations, such as land surface temperature~~LST~~, the geostationary satellite FY-2C was used to retrieve plateau-scale land surface temperatures~~LST~~. Other parameters with typical diurnal characteristics, such as downward longwave and shortwave radiation, air temperature, specific humidity, wind speed and air pressure, were derived from ITPCAS meteorological forcing data. Based on the SEBS model and the above inputs, a time series of hourly land atmosphere~~surface~~ heat flux data over the TP was derived using a combination of geostationary and polar orbiting satellite data. The new dataset has a fine spatial resolution of 10 km. According to the validation with 6 field stations (more than 3800 samples), the high correlation coefficients and low RMSEs indicate that the estimated land surface heat fluxes are in good agreement with the ground truth. Furthermore, the estimates were also compared with the GLDAS flux data, which were thought to have high accuracy~~quality~~. The results showed that most derived variables were superior to the GLDAS data. Based on this new dataset, the diurnal cycle of land surface heat fluxes was clearly identified. Moreover, the seasonal variations were found to be

influenced by the Asian monsoon system. This new dataset can help to understand and quantify the diurnal variations in the land surface heating field, which are very important for atmospheric circulation and weather changes in the TP, especially in winter and spring when the main heating source is from the land surface. This dataset can also help to evaluate the results of numerical models.

- 5      The uncertainties of input forcing data, the accuracy of land surface parameters from satellite retrievals, the mismatch between different scales and some assumptions and simplification in the SEBS model itself lead to some discrepancies between the estimation and observation. Thanks to Because of the relatively homogeneous land surface statusconditions of the field stations, the spatial scale mismatch between different data should have been minimized in our study. Scintillometry is possibly the most convenient method to measure fluxes at a scale of 1-10 km-scale. Unfortunately, this device is lacking over the TP. If we have enough in-situ measurements within a grid scale of 10 km or 25 km, an average or weighted average of measurements can be directly used to reduce some uncertainties caused by scale mismatch. However, for well-known reasons, it is very difficult to carry out such measurements in the TP with the harsh environment and climate conditions. For the next step, it is
- 10     worthwhile to examine subpixel surface heat fluxes using techniques such as the temperature-sharpening method. Additionally, the FY-4 satellite with much higher spatial, temporal and spectral resolution will provide the opportunity to monitor land-atmosphere interactions in much more detail.
- 15

- 20     **Data availability.** The ground-based measurements used in this study were obtained from the Third Pole Environment Database (<http://www.tpedatabase.cn/portal/MetaDataInfo.jsp?MetaDataId=43>). The SPOT data can be downloaded from <https://www.vito-eodata.be/PDF/portal/Application.html>. The FY-2C data can be downloaded from <http://satellite.nsdc.org.cn/portalsite/Data/DataView.aspx>. The forcing data set for this study can be obtained from <http://dam.itpcas.ac.cn/chs/rs/?q=data>.

25

**Author contributions.** LZ designed the study and performed the SEBS model with help from YM and ZH. XW, MC and NG collected the analyzed the in-situ flux data and forcing data. YH and LZ retrieved the land surface parameters from FY-2C and SPOT data. LZ wrote the manuscript with help from YM and YF. All commented on the paper.

30

**Competing interests.** The authors declare that they have no conflict of interest.

**Acknowledgements.** This research was jointly funded by Strategic Priority Research Program of Chinese Academy of Sciences (Grant No. XDA20060101), the National Natural Science Foundation of China (Grant No. 41875031, 41522501, 41275028, 41661144043), the Chinese Academy of Sciences (Grant No. QYZDJ-SSW-DQC019) and CLIMATE-TPE (ID 32070) in the framework of the ESA-MOST Dragon 4 Programme. [We would like to thank the three anonymous reviewers for their valuable comments.](#)

10      **References**

[Abdolghafoorian, A., Farhadi, L., Batani, S.M., Margulis, S., Xu, T.R.: Characterizing the effect of vegetation dynamics on the bulk heat transfer coefficient to improve variational estimation of surface turbulent fluxes. J. Hydrometeorol. 18, 321-333, 2017.](#)

Allen, R. G., Tasumi, M., Morse, A., Trezza, R., Wright, J. L., Bastiaanssen, W., Kramber, W., Lorite, I.,  
15      and Robison, C. W.: Satellite-based energy balance for mapping evapotranspiration with internalized calibration (METRIC) - Applications. J. Irrig. Drain. Eng., 133(4), 395-406, DOI:  
10.1061/(ASCE)0733-9437(2007)133:4(395), 2007.

Bastiaanssen, W. G., Menenti, M., Feddes, R. A., and Holtslag, A. A. M.: A remote sensing surface energy balance algorithm for land (SEBAL). 1. Formulation. J. Hydrol., 212, 198-212, DOI:  
20      10.1016/S0022-1694(98)00253-4, 1998.

[Batani, S.M., Entekhabi, D., and Castelli, F.: Mapping evaporation and estimation of surface control of evaporation using remotely sensed land surface temperature from a constellation of satellites. Water Resour. Res., 49, 950-968, DOI:10.1002/wrcr.20071, 2013.](#)

Boos, W. R., and Kuang, Z. M.: Dominant control of the South Asian monsoon by orographic  
25      insulation versus plateau heating. Nature, 463, 218-223, DOI: 10.1038/nature08707, 2010.

Boos, W. R., and Kuang, Z. M.: Sensitivity of the south Asian monsoon to elevated and non-elevated  
heating. Sci. Rep., 3(1192), DOI: 10.1038/srep01192, 2013.

Chen, X., Su, Z., Ma, Y., Yang, K., Wen, J., and Zhang, Y.: An improvement of roughness height  
parameterization of the Surface Energy Balance System (SEBS) over the Tibetan Plateau. J. Appl.

30      Meteorol. Clim., 52(3), 607-622, DOI: 10.1175/JAMC-D-12-056.1, 2013a.

Chen, X., Su, Z., Ma, Y., Yang, K., and Wang, B.: Estimation of surface energy fluxes under complex terrain of Mt. Qomolangma over the Tibetan Plateau. *Hydrol. Earth Syst. Sc.*, 17(4), 1607-1618, DOI: 10.5194/hess-17-1607-2013, 2013b.

5 [Crow, W.T., and Kustas, W.P.: Utility of assimilating surface radiometric temperature observations for evaporative fraction and heat transfer coefficient retrieval. \*Bound-Lay. Meteorol.\*, 115\(1\), 105-130, DOI:10.1007/s10546-004-2121-0, 2005.](#)

[Foken, T., Göckede, M., Mauder, M., Mahrt, L., Amiro, B., Munger, W.: Post-Field Data Quality Control. In: Lee, X., Massman, W., Law, B. \(eds\) \*Handbook of Micrometeorology. Atmospheric and Oceanographic Sciences Library\*, 29, 181-208, Springer, Dordrecht, 2004.](#)

10 [Foken, T., and Wichura, B.: Tools for quality assessment of surface-based flux measurements. \*Agri. For. Meteorol.\*, 78, 83-105, 1996.](#)

He, J.: Development of surface meteorological dataset of China with high temporal and spatial resolution, M.S. thesis, Inst. of Tibetan Plateau Res., Chin. Acad. of Sci., Beijing, China, 2010.

15 Hu, Y., Zhong, L., Ma, Y., Zou, M., Xu, K., Huang, Z., and Feng, L.: Estimation of the land surface temperature over the Tibetan Plateau by using Chinese FY-2C geostationary satellite data. *Sensors*, 18, 376, DOI: 10.3390/s18020376, 2018.

Jia, L., Su, Z., van den Hurk, B., Menenti, M., Moene, A., De, Bruin H. A. R., Yrisarry, J. J. B., Ibanez, M., and Cuesta, A.: Estimation of sensible heat flux using the Surface Energy Balance System (SEBS) and ATSR measurements. *Phys. Chem. Earth, Parts A/B/C*, 28(1-3), 75-88, DOI: 10.1016/S1474-7065(03)00009-3, 2003.

20 [Lee, X., and Hu, X.: Forest air fluxes of carbon, water and energy over non flat terrain. \*Bound. Lay. Meteorol.\*, 103\(2\), 277-301, DOI: 10.1023/A:1014508928693, 2002](#)

Liu, X., and Chen, B.: Climatic warming in the Tibetan Plateau during recent decades. *Int. J. Climatol.*, 20(14), 1729-1742, 2000.

25 [Ma W, Ma, Y. and Ishikawa, H.: Evaluation of the SEBS for upscaling the evapotranspiration based on in-situ observations over the Tibetan Plateau. \*Atmos. Res.\*, 138, 91-97, 2014.](#)

Ma, W., Ma, Y., Li, M., Hu, Z., Zhong, L., Su, Z., Ishikawa, H., and Wang, J.: Estimating surface fluxes over the north Tibetan Plateau area with ASTER imagery. *Hydrol. Earth Syst. Sc.*, 13(1), 57-67, DOI: 10.5194/hess-13-57-2009, 2009.

30 Ma, Y., Ma, W., Zhong, L., Hu, Z., Li, M., Zhu, Z., Han, C., Wang, B., and Liu, X.: Monitoring and

modeling the Tibetan Plateau's climate system and its impact on east Asia. *Sci. Rep.*, 7, 44574 , DOI: 10.1038/srep44574, 2017.

Ma, Y., Menenti, M., Feddes, R. A., and Wang, J.: The analysis of the land surface heterogeneity and its impact on atmospheric variables and the aerodynamic and thermodynamic roughness lengths. *J. Geophys. Res.-Atmos.*, 113, D08113, DOI: 10.1029/2007JD009124, 2008.

5 Ma, Y., Su, Z., Koike, T., Yao, T., Ishikawa, H., Ueno, K. I., and Menenti, M.: On measuring and remote sensing surface energy partitioning over the Tibetan Plateau—from GAME/Tibet to CAMP/Tibet. *Phys. Chem. Earth*, 28(1-3), 63-74, DOI: 10.1016/S1474-7065(03)00008-1, 2003.

Ma, Y., Su, Z., Li, Z., Koike, T., and Menenti, M.: Determination of regional net radiation and soil heat flux over a heterogeneous landscape of the Tibetan Plateau. *Hydrol. Process.*, 16(15), 2963-2971, DOI: 10.1002/hyp.1079, 2002.

10 Ma, Y., Zhong, L., Su, Z., Ishikawa, H., Menenti, M., and Koike, T.: Determination of regional distributions and seasonal variations of land surface heat fluxes from Landsat-7 Enhanced Thematic Mapper data over the central Tibetan Plateau area. *J. Geophys. Res.-Atmos.*, 111, D10305, DOI: 15 10.1029/2005JD006742, 2006.

[Majozi, N. P., Mannaerts, C. M., Ramoelo, A., Mathieu, R. S., Nickless, A., and Verhoef, W.: Analysing surface energy balance closure and partitioning over a semi-arid savanna FLUXNET site in Skukuza, Kruger National Park, South Africa. \*Hydrol. Earth Syst. Sc.\*, 21\(7\), 3401-3415, DOI: 10.5194/hess-21-3401-2017, 2017.](#)

20 [Mauder, M., Onceley, S. P., Vogt, R., Weidinger, T., Ribeiro, L., Bernhofer, C., Foken, T., Kohsiek, W., De Bruin HAR., and Liu, H.: The energy balance experiment EBEX 2000. Part II: Intercomparison of eddy covariance sensors and post field data processing methods. \*Bound. Lay. Meteorol.\*, 123\(1\), 29-54, DOI: 10.1007/s10546-006-9139-4, 2007.](#)

Norman, J., Kustas, W. P., and Humes, K. S.: Source approach for estimating soil and vegetation energy fluxes in observations of directional radiometric surface temperature. *Agr. Forest Meteorol.*, 25 77(3-4), 263-293, DOI: 10.1016/0168-1923(95)02265-Y, 1995.

Oku, Y., and Ishikawa, H.: Estimation of land surface temperature over the Tibetan Plateau using GMS data. *J. Appl. Meteorol.*, 43, 548-561, 2004.

30 Oku, Y., Ishikawa, H., Haginoya, S., and Su, Z.: Estimation of land surface heat fluxes over the Tibetan Plateau using GMS data. *J. Appl. Meteorol. Clim.*, 46, 183-195, 2007.

- Pan, X., Liu, Y., Fan, X., and Gan, G.: Two energy balance closure approaches: applications and comparisons over an oasis desert ecotone. *J. Arid Land*, 9(1), 51-64, DOI: [10.1007/s40333-016-0063-2](https://doi.org/10.1007/s40333-016-0063-2), 2017.
- Qiu, J.: Monsoon Melee. *Science*, 340(6139), 1400-1401, DOI: [10.1126/science.340.6139.1400](https://doi.org/10.1126/science.340.6139.1400), 2013.
- 5 Rodell, M., Houser, P. R., Jambor, U., Gottschalck, J., Mitchell, K., Meng, C. J., Arsenault, K., Cosgrove, B., Radakovich, J., Bosilovich, M., Entin, J. K., Walker, J. P., Lohmann, D., and Toll, D.: The Global Land Data Assimilation System. *B. Am Meteorol. Soc.*, 85(3), 381-394, DOI: [10.1175/BAMS-85-3-381](https://doi.org/10.1175/BAMS-85-3-381), 2004.
- Roerink, G. J., Su, Z., and Menenti, M.: S-SEBI: A simple remote sensing algorithm to estimate the 10 surface energy balance. *Phys. Chem. Earth, Part B: Hydrology, Oceans and Atmosphere*, 25(2), 147-157, DOI: [10.1016/S1464-1909\(99\)00128-8](https://doi.org/10.1016/S1464-1909(99)00128-8), 2000.
- Sánchez, J. M., Scavone, G., Caselles, V., Valor, E., Copertino, V. A., and Telesca, V.: Monitoring daily evapotranspiration at a regional scale from Landsat-TM and ETM+ data: Application to the Basilicata region. *J. Hydrol.*, 351(1-2), 58-70, DOI: [10.1016/j.jhydrol.2007.11.041](https://doi.org/10.1016/j.jhydrol.2007.11.041), 2008.
- 15 Seneviratne, S. I., and Stöckli, R.: The role of land-atmosphere interactions for climate variability in Europe [C]. *Climate Variability and Extremes During the Past 100 years*, Switzerland, Springer, 179-193, 2008.
- Su, Z.: The Surface Energy Balance System (SEBS) for estimation of turbulent heat fluxes. *Hydrol. Earth Syst. Sc.*, 6(1), 85-100, DOI: [10.5194/hess-6-85-2002](https://doi.org/10.5194/hess-6-85-2002), 2002.
- 20 Twine, T. E., Kustas, W. P., Norman, J. M., Cook, D. R., Houser, P., Meyers, T. P., Prueger, J. H., Starks, P. J., and Wesely, M. L.: Correcting eddy covariance flux underestimates over a grassland. *Agr. Forest Meteorol.*, 103(3), 279-300, DOI: [10.1016/S0168-1923\(00\)00123-4](https://doi.org/10.1016/S0168-1923(00)00123-4), 2000.
- Wilson, K., Goldstein, A., Falge, E., Aubinet, M., Baldocchi, D., Berbigier, P., Bernhofer, C., Ceulemans, R., Dolman, H., Field, C., Grelle, A., Ibrom, A., Law, B. E., Kowalski, A., Meyers, T., 25 Moncrieff, J., Monson, R., Oechel, W., Tenhunen, J., Valentini, R., and Verma, S.: Energy balance closure at FLUXNET sites. *Agr. Forest Meteorol.*, 113(1), 223-243, DOI: [10.1016/S0168-1923\(02\)00109-0](https://doi.org/10.1016/S0168-1923(02)00109-0), 2002.
- Wolf, A., Saliendra, N., Akshakov, K., Johnson, D. A., and Laca, E.: Effects of different eddy covariance correction schemes on energy balance closure and comparisons with the modified Bowen ratio system. *Agr. Forest Meteorol.*, 148(6-7), 942-952, DOI: [10.1016/j.agrformet.2008.07.010](https://doi.org/10.1016/j.agrformet.2008.07.010), 2008.

[10.1016/j.agrformet.2008.01.005, 2008.](https://doi.org/10.1016/j.agrformet.2008.01.005)

Wu, G., Duan, A., Liu, Y., Mao, J., Ren, R., Bao, Q., He, B., Liu, B., and Hu, W: Tibetan Plateau climate dynamics: recent research progress and outlook. *Natl. Sci. Rev.*, 2, 100-116, DOI: 10.1093/nsr/nwu045, 2015.

5 Wu, G., Liu, Y., He, B., Bao, Q., Duan, A., and Jin, F.: Thermal controls on the Asian summer monsoon. *Sci. Rep.*, 2, 404, DOI: 10.1038/srep00404, 2012.

Xu, T.R., Bateni, S.M., Liang, S.L., Entekhabi, D., and Mao, K.B.: Estimation of surface turbulent heat fluxes via variational assimilation of sequences of land surface temperatures from Geostationary Operational Environmental Satellites. *J. Geophys. Res.*, 119, 10,780-10,798, doi:10.1002/2014JD021814, 2014.

Xu, T.R., He, X.L., Bateni, S.M., Auligne, T., Liu, S.M., Xu, Z.W., Zhou, J., and Mao, K.B.: Mapping regional turbulent heat fluxes via variational assimilation of land surface temperature data from polar orbiting satellites. *Remote Sens. Environ.*, 221, 444-461, <https://doi.org/10.1016/j.rse.2018.11.023>, 2019.

15 Yang, K., and Wang, J.: A temperature prediction-correction method for estimating surface soil heat flux from soil temperature and moisture data. *Sci. China Ser. D: Earth Sciences*, 51(5), 721-729, DOI: 10.1007/s11430-008-0036-1, 2008.

Yang, K., He, J., Tang, W., Qin, J., and Cheng, CCK.: On downward shortwave and longwave radiations over high altitude regions: Observation and modeling in the Tibetan Plateau. *Agric. Forest Meteorol.*, 150, 38-46, 2010.

Ye, D., and Gao, Y.: Meteorology of the Qinghai-Xizang (Tibet) Plateau. Science Press, 278 pp, 1979.

Zhong, L., Ma, Y., Fu, Y., Pan, X., Hu, W., Su, Z., Salama, M.S., and Feng, L.: Assessment of soil water deficit for the middle reaches of Yarlung-Zangbo River from optical and passive microwave images. *Remote Sens. Environ.*, 142, 1-8, DOI: 10.1016/j.rse.2013.11.008, 2014.

25 Zhong, L., Ma, Y., Su, Z., and Salama, M.S.: Estimation of land surface temperature over the Tibetan Plateau using AVHRR and MODIS data. *Adv. Atmos. Sci.*, 27(5): 1110-1118, DOI: 10.1007/s00376-009-9133-0, 2010.

Zhong, L., Su, Z., Ma, Y., Salama, M. S., and Sobrino, J. A.: Accelerated changes of environmental conditions on the Tibetan Plateau caused by climate change. *J. Climate*, 24(4): 6540-6550, DOI: 10.1175/JCLI-D-10-05000.1, 2011.

Zou, M., Zhong, L., Ma, Y., Hu, Y., and Feng, L.: Estimation of actual evapotranspiration in the Nagqu river basin of the Tibetan Plateau. *Theor. Appl. Climatol.*, 132(3-4), 1039-1047, DOI: 10.1007/s00704-017-2154-1, 2017.

Zou, M., Zhong, L., Ma, Y., Hu, Y., Huang, Z., Xu, K., and Feng, L.: Comparison of two satellite-based evapotranspiration models of the Nagqu River Basin of the Tibetan Plateau. *J. Geophys. Res.-Atmos.*, 123, 3961–3975, DOI: 10.1002/2017JD027965, 2018.

10

15

20

25

30

**Table 1:** Ground measurement sites.

Sites	Longitude (E)	Latitude (N)	Elevation (m)	Land cover
BJ	91.899	31.369	4509.0	Plateau meadow
D105	91.943	33.064	5039.0	Plateau grassland
MS3478	91.716	31.926	4620.0	Plateau meadow
Linzhi	94.738	29.765	3326.0	Slope grassland
Nam Co	90.989	30.775	4730.0	Plateau grassland
QOMS	86.946	28.358	4276.0	Gravels

**Table 2:** Summary of the input datasets used for calculating land surface heat fluxes.

Variables	Data Source	Resolution	
		Spatial	Temporal
$T_s$	FY-2C/SVISSR	5 km	hourly
NDVI	SPOT/VGT	1 km	daily
$P_v$	SPOT/VGT	1 km	daily
$\alpha$	SPOT/VGT	1 km	daily
$\varepsilon_s$	SPOT/VGT	1 km	daily
$R_{swd}$	ITPCAS	10 km	3-hour
$R_{lwd}$	ITPCAS	10 km	3-hour
u	ITPCAS	10 km	3-hour
$T_a$	ITPCAS	10 km	3-hour
SH	ITPCAS	10 km	3-hour
$P_s$	ITPCAS	10 km	3-hour

**Table 3: The validation of the forcing data.**

Variables	RMSE	MB	MAE	R	N
$R_{swd}$ ( $\text{W}\cdot\text{m}^{-2}$ )	68.50	-4.73	37.38	0.974	1048
$R_{lwd}$ ( $\text{W}\cdot\text{m}^{-2}$ )	20.98	-8.49	16.98	0.954	1048
$u$ ( $\text{m}\cdot\text{s}^{-1}$ )	1.71	-1.01	1.28	0.793	1440
$T_a$ (K)	2.08	-0.045	1.08	0.975	1440
$SH$ ( $\text{kg}\cdot\text{kg}^{-1}$ )	$0.56\times10^{-3}$	$-0.76\times10^{-4}$	$0.37\times10^{-3}$	0.981	1438
$P_s$ (hPa)	8.51	-2.25	6.53	0.865	1440

**Table 4: Comparison of derived flux data product and GLDAS against in situ measurements (Units:  $\text{Wm}^{-2}$ ).**

Model	Indicators	Rn	H	LE	G <sub>0</sub>	SWU	LWU
<b>SEBS</b>	<b>RMSE</b>	76.63	60.29	<u>71.03</u>	37.5	49.81	52.99
	<b>MB</b>	-3.11	-22.13	<u>8.01</u>	7.81	11.74	-34.93
	<b>MAE</b>	50.49	45.67	<u>48.79</u>	28.43	26.88	39.31
	<b>R</b>	0.935	0.789	<u>0.772</u>	0.791	0.900	0.798
	<b>N</b>	4720	4554	3865	3837	4898	4721
<b>GLDAS</b>	<b>RMSE</b>	114.32	67.77	75.60	40.05	56.97	45.18
	<b>MB</b>	23.43	27.88	-10.35	-4.00	-15.42	-28.06
	<b>MAE</b>	81.90	47.48	44.89	30.52	31.35	31.61
	<b>R</b>	0.836	0.807	0.660	0.755	0.779	0.870
	<b>N</b>	1633	1580	1341	1329	1633	1633

**Table 5: Uncertainties for each meteorological forcing variable and the induced changes in  $H_s$  and LE.**

Variables	Assumed Uncertainty	Induced Uncertainty of $H_s$	Induced Uncertainty of LE
$R_{swd}$ ( $\text{W}\cdot\text{m}^{-2}$ )	<u>-68.50~68.5</u>	<u>-12.34~6.22</u> ( <u>-8.05%~4.06%</u> )	<u>-29.75~35.86</u> ( <u>-17.92%~21.60%</u> )
$R_{lwd}$ ( $\text{W}\cdot\text{m}^{-2}$ )	<u>-20.98~20.98</u>	<u>-2.50~2.50</u> ( <u>-1.63%~1.63%</u> )	<u>-15.54~15.54</u> ( <u>-9.36%~9.36%</u> )
$u$ ( $\text{m}\cdot\text{s}^{-1}$ )	<u>-1.71~1.71</u>	<u>-9.47~7.31</u> ( <u>-6.18%~4.77%</u> )	<u>9.47~7.31</u> ( <u>5.71%~4.41%</u> )
$T_a$ (K)	<u>-2.08~2.08</u>	<u>14.64~16.94</u> ( <u>9.55%~-11.05%</u> )	<u>-14.64~16.94</u> ( <u>-8.82%~10.20%</u> )
$SH$ ( $\text{kg}\cdot\text{kg}^{-1}$ )	<u><math>-0.56\times10^{-3}</math>~<math>0.56\times10^{-3}</math></u>	<u>-0.01~0.01</u> ( <u>-0.01%~0.01%</u> )	<u>0.01~0.01</u> ( <u>0.01%~-0.01%</u> )
$P_s$ (hPa)	<u>-8.51~8.51</u>	<u>-0.01~0.01</u> ( <u>-0.01%~0.01%</u> )	<u>0.01~0.01</u> ( <u>0.01%~-0.01%</u> )

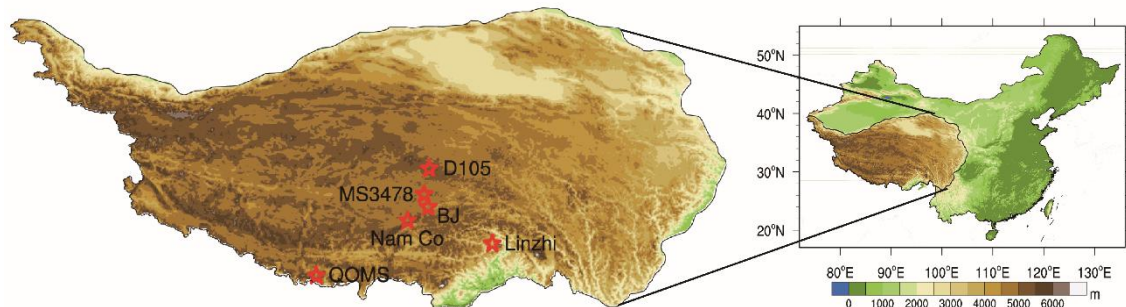


**Figure 1: Location of the Tibetan Plateau.** [The right panel illustrates the location of the Tibetan Plateau in China.](#) [The left panel shows the spatial distribution of eddy-covariance stations.](#) The pentagrams represent the eddy-covariance stations in the Tibetan Plateau. [The legend of the color map indicates the altitude elevation –above mean sea level in meters.](#)

5

10

15

20

25

30

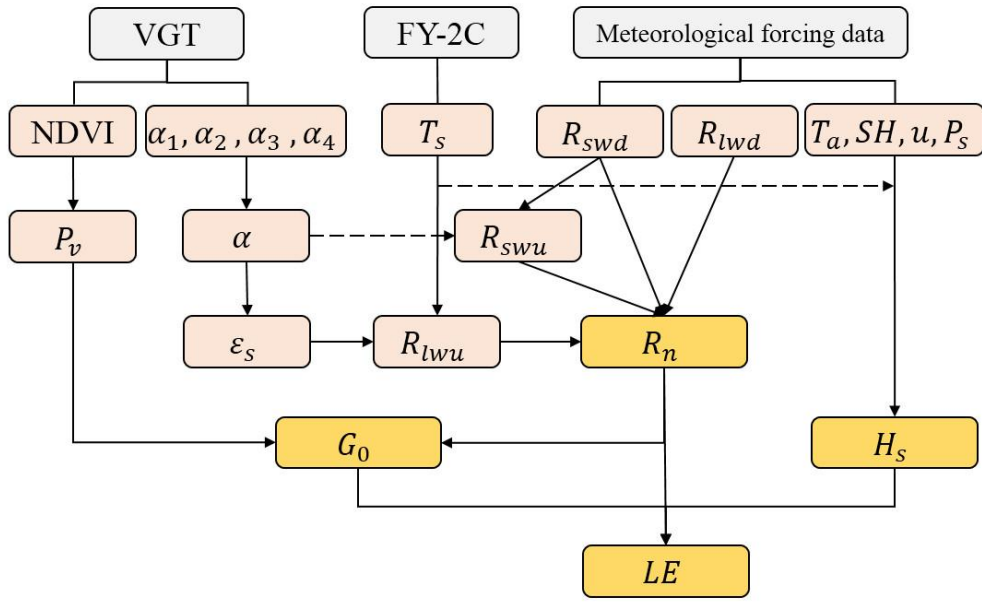


**Figure 2: Flowchart of the flux estimation method [to determine the net radiation flux, sensible heat flux, latent heat flux by combining VGT, FY-2C and meteorological forcing data.](#)**

5

10

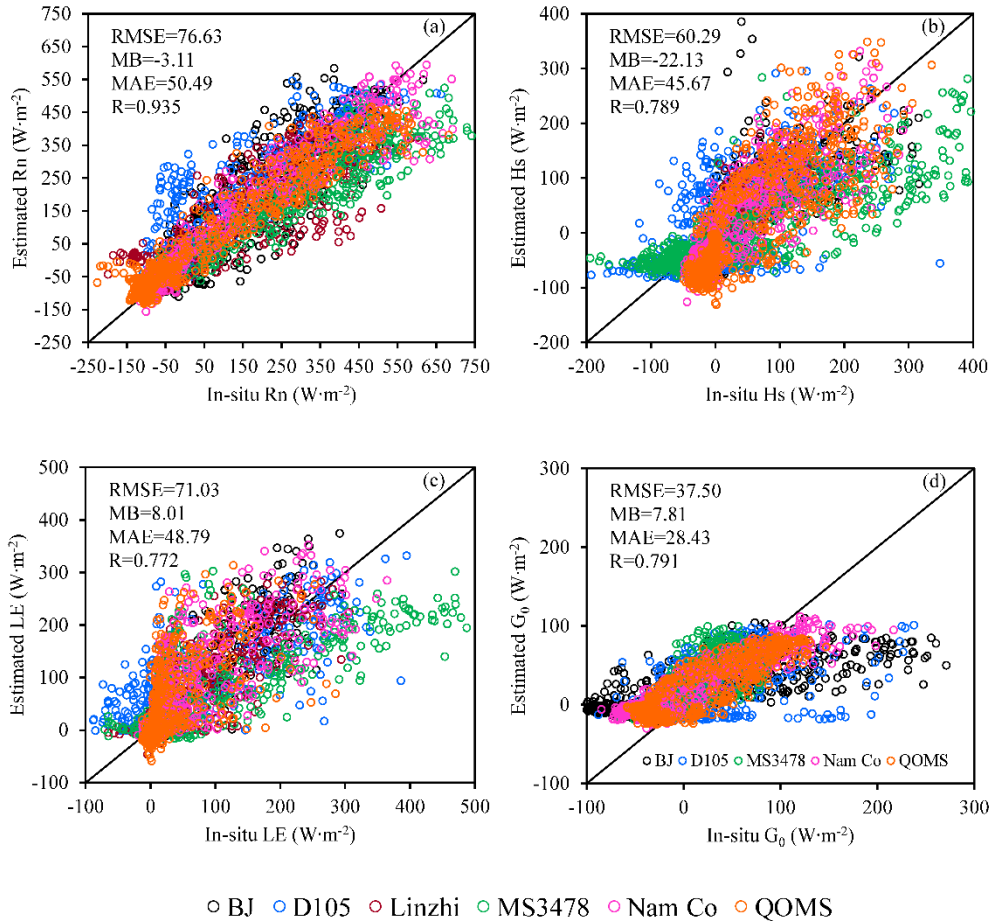


**Figure 3: Validation of surface heat fluxes estimated by the SEBS model with in situ measurements (a. Net radiation flux; b. Sensible heat flux; c. Latent heat flux; d. Soil heat flux). [The legend of with different colors indicates the six stations \(BJ, D105, Linzhi, MS3478, Nam Co and QOMS\) involved in the validation.](#)**

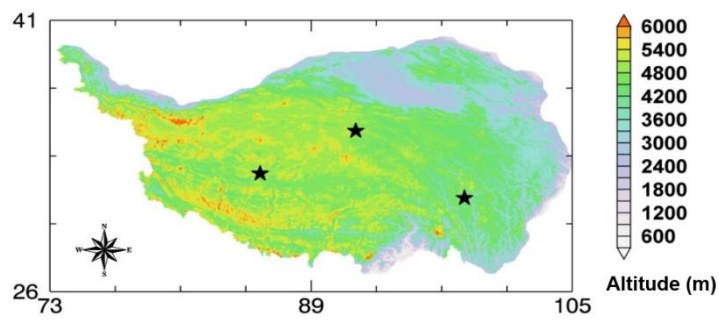


**Figure 4: The locations of the three sites (marked by pentagrams) for carrying out sensitivity tests of input-meteorological forcing input data. The legend of the color map indicates the altitude elevation above mean sea level in meters.**

5

10

15

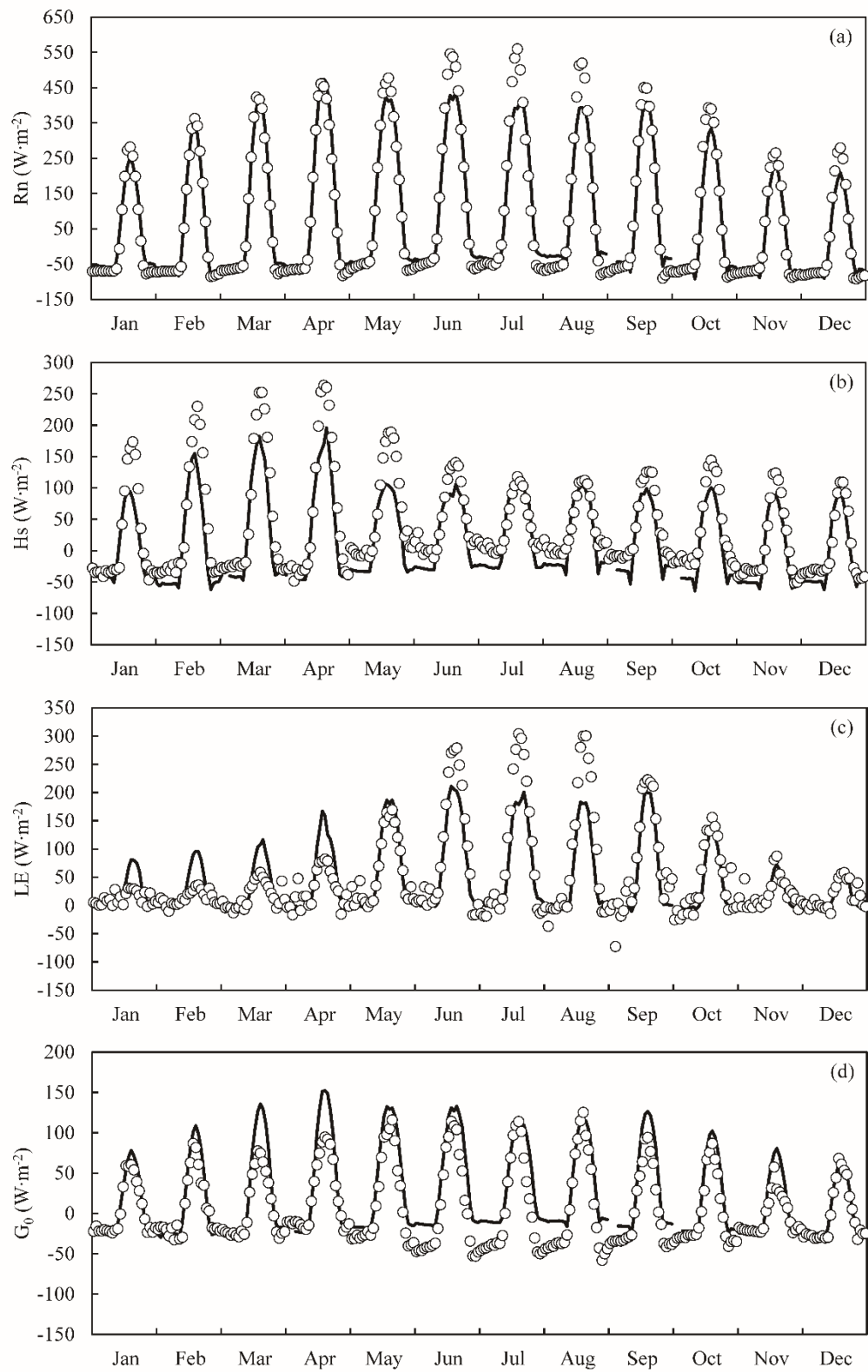


**Figure 5: Time series of monthly mean diurnal change in surface energy fluxes (units: Wm-2) observed by in situ measurements (circles) and those estimated by using the SEBS model (curves) at the BJ station in 2008 (a. net radiation flux; b. sensible heat flux; c. latent heat flux; d. soil heat flux).**

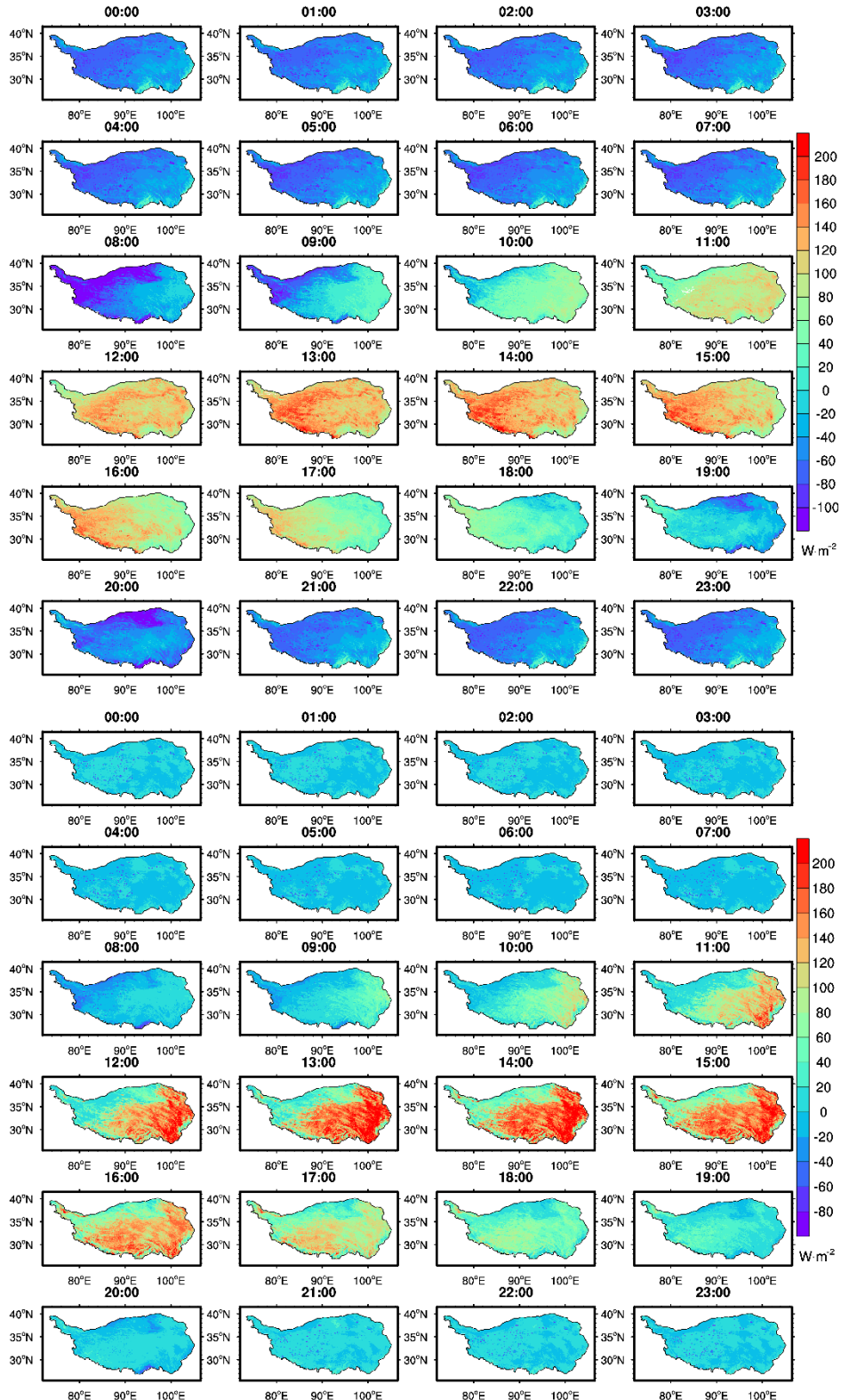


**Figure 6:** The anual mean spatial distribution and diurnal cycle of sensible heat flux (top panels) and latent heat flux (bottom panels) in 2008 over the TP.